Beamline studies of block copolymer self-assembly and magnetic materials

Caroline A. Ross
Li-Chen Cheng, Kun-Hua Tu, Sangho Lee, John Simonaitis, Wubin Bai, Adam Hannon, Ethan Rosenberg, Andy Quindeau, Shuchi Ojha
Dept. of Materials Science and Engineering, MIT
Kevin Yager
Brookhaven National Laboratory

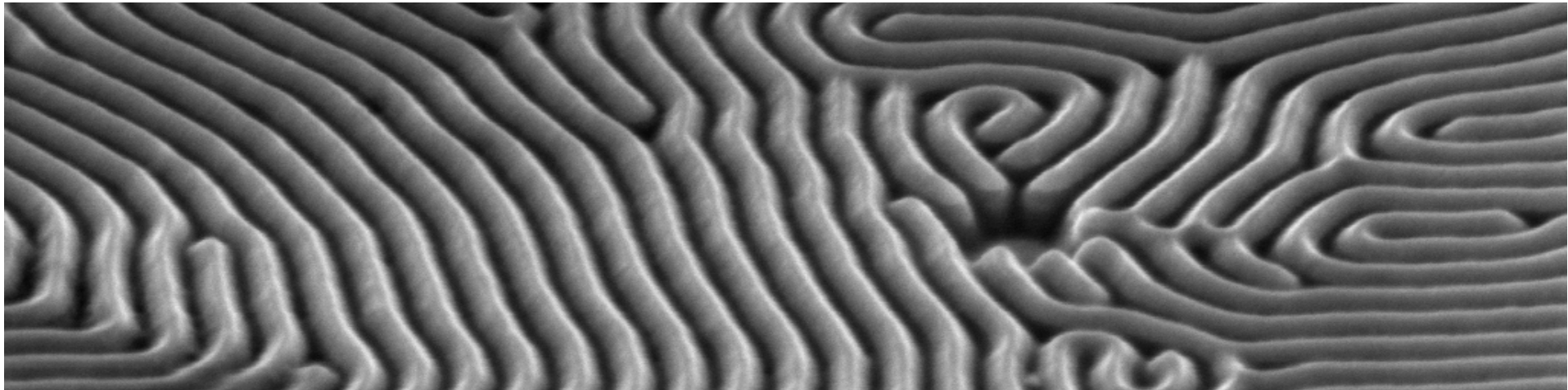

Block Copolymer Self-assembly for Nanofabrication

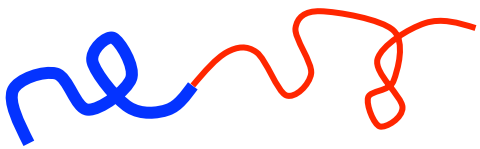

diblock copolymer

triblock terpolymer

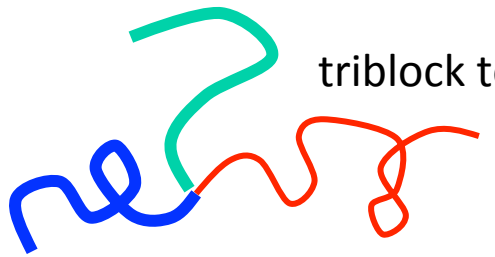

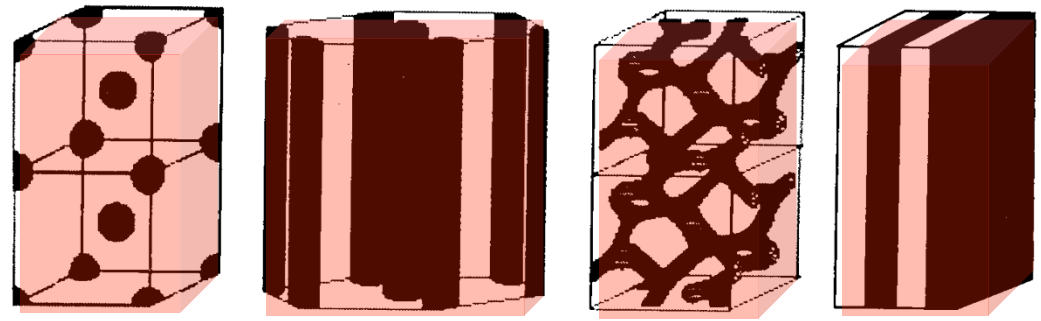

Spheres **Cylinders** Gyroids Lamellae

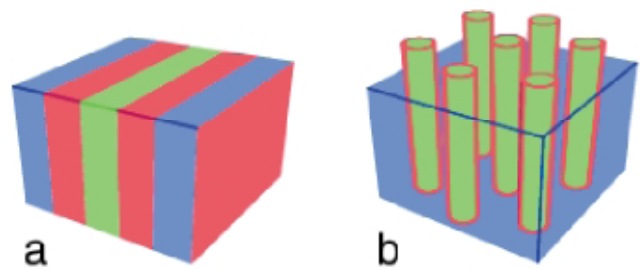

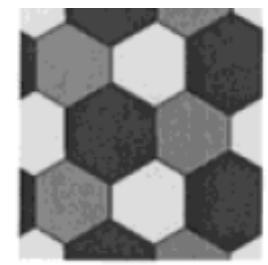

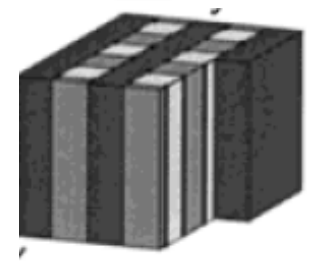

Block copolymers could be used as 'self assembled resists' with half-pitch as low as ~3 nm. Templating imparts long range order.

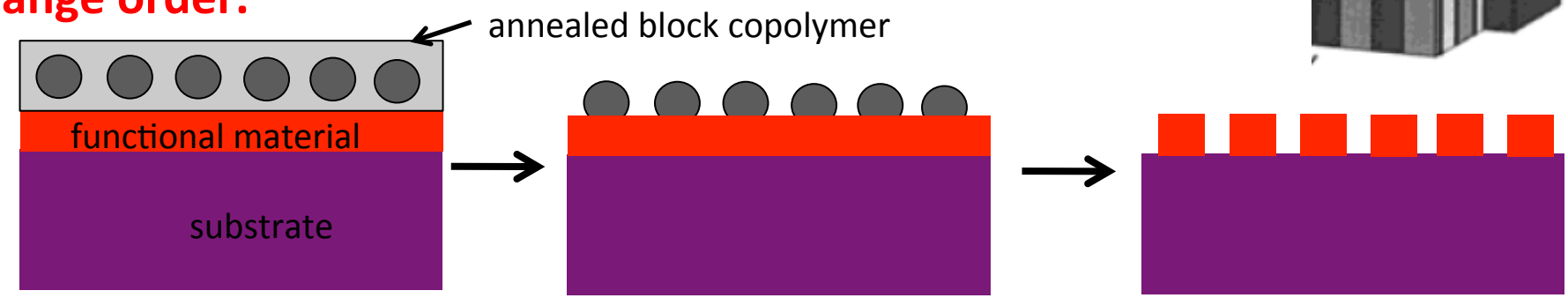

Bates and Fredrickson, *Annu. Rev. Phys. Chem.* **41**, 525 (1990); Bates, et al. *Phys. Today* (1999), **52**, 32.

Topographical Templating of BCP Films

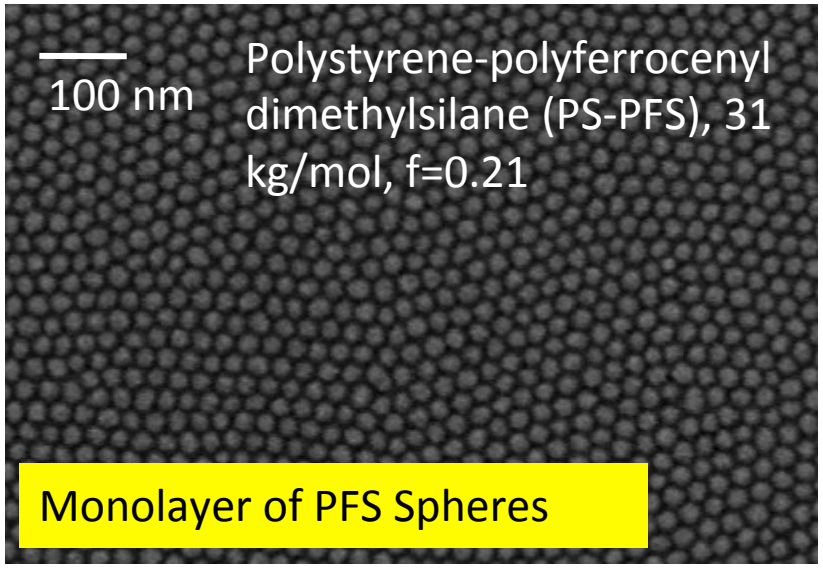

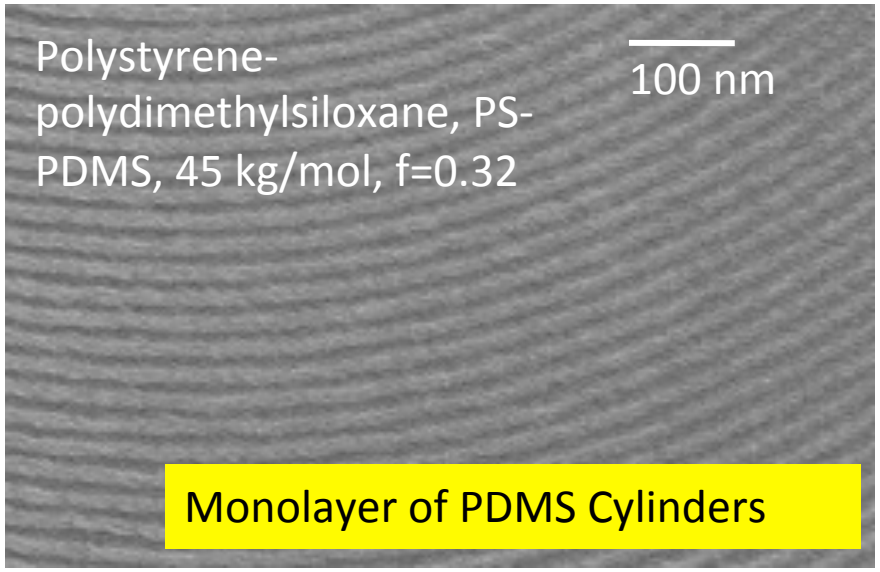

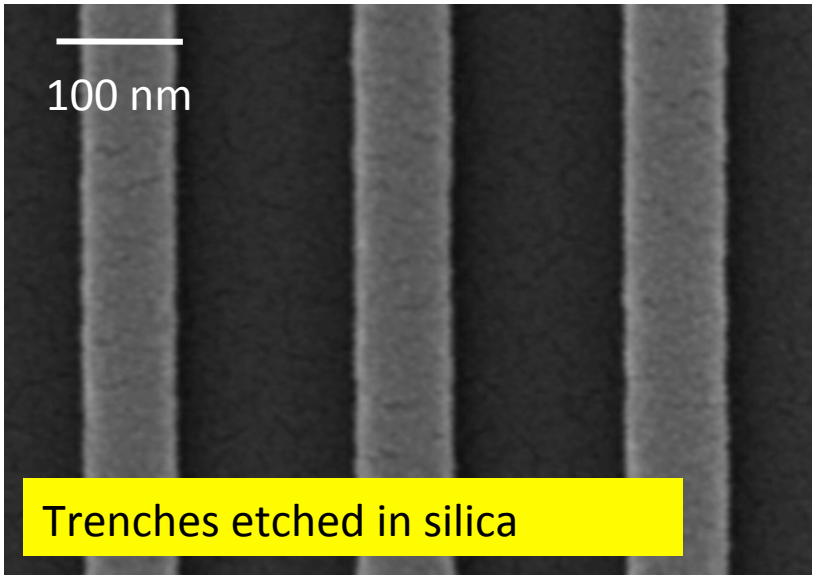

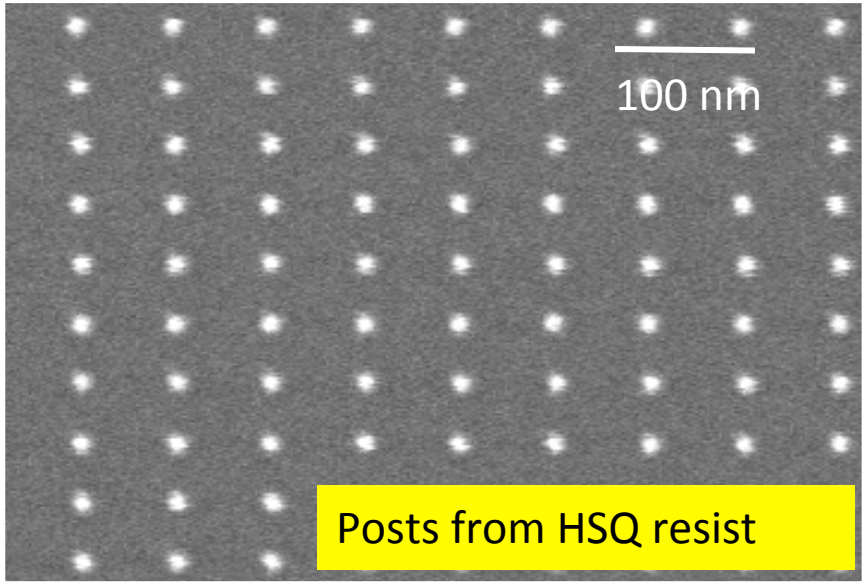

Templates can be **chemical** (e.g. Russell, PRL 82 2602 1999, Nealey, Science, 308, 1442 2005) or **topographical** (Kramer, Adv Mater. 13 1152 2001) modulations in the surface of the substrate.

Templating using trenches

Spherical PS-PFS

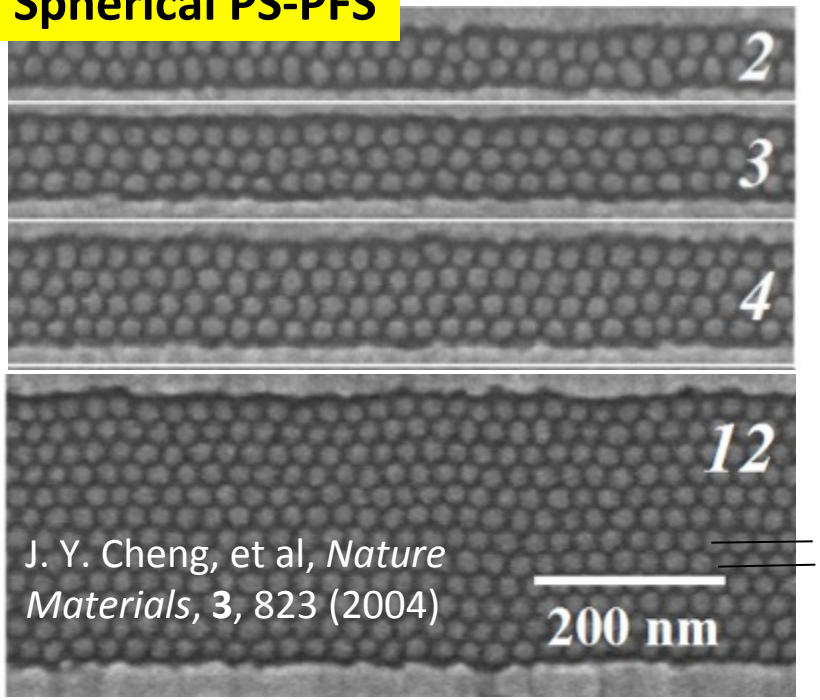

J. Y. Cheng, et al, *Nature Materials*, **3**, 823 (2004)

L_o

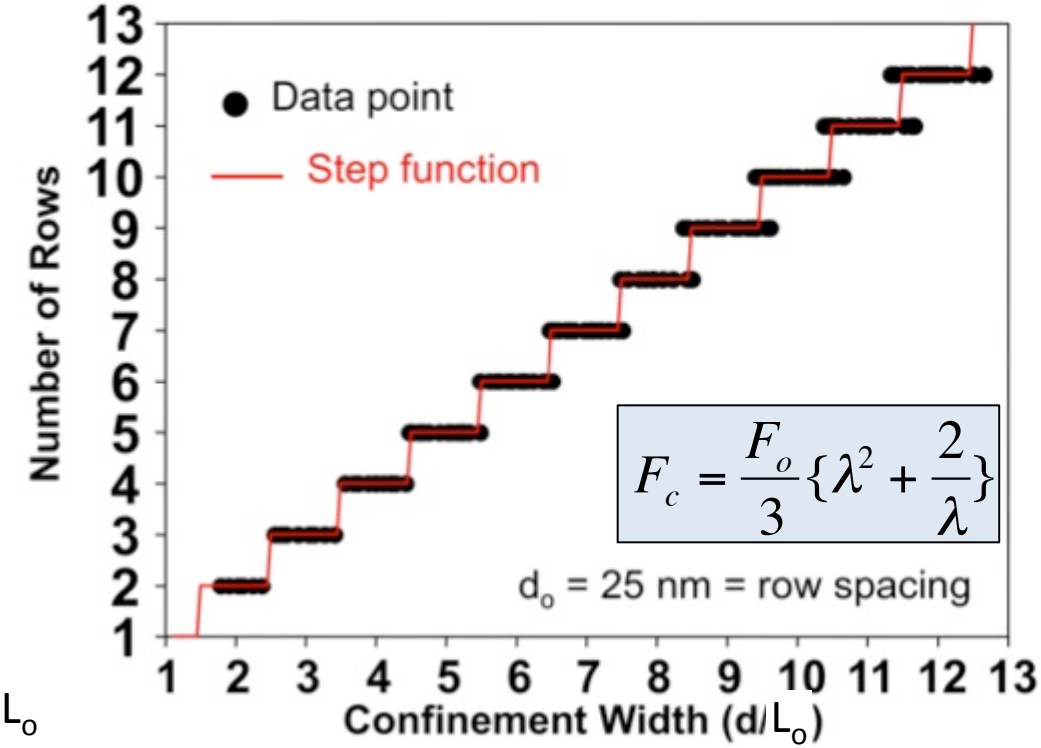

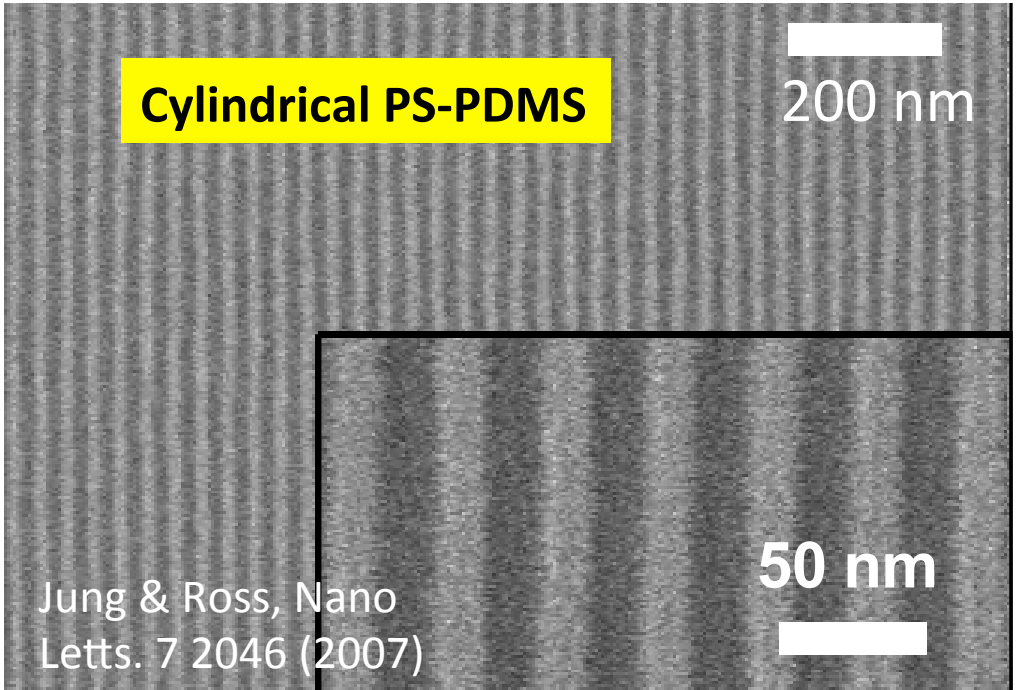

Jung & Ross, Nano Letts. 7 2046 (2007)

- Template imparts long range order
- Number of features within template is determined by commensurability between template and the block copolymer period L_0.

Templating using posts

Monolayer of Spheres

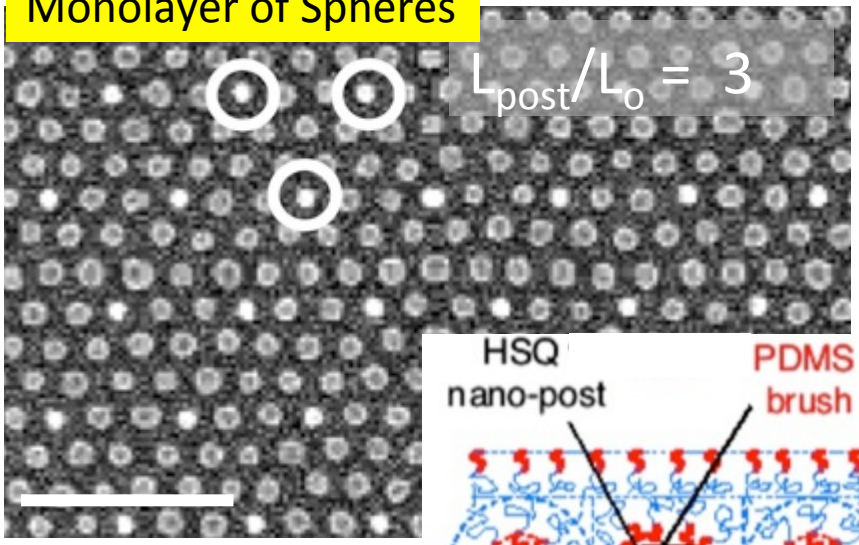

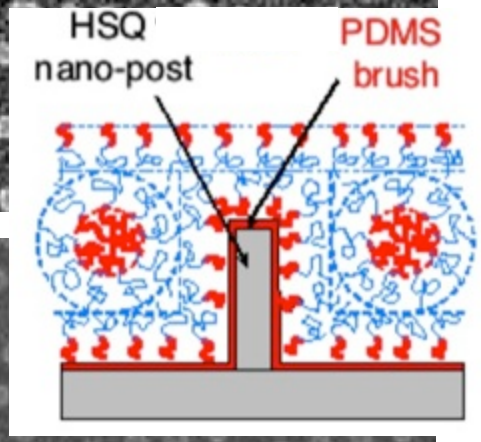

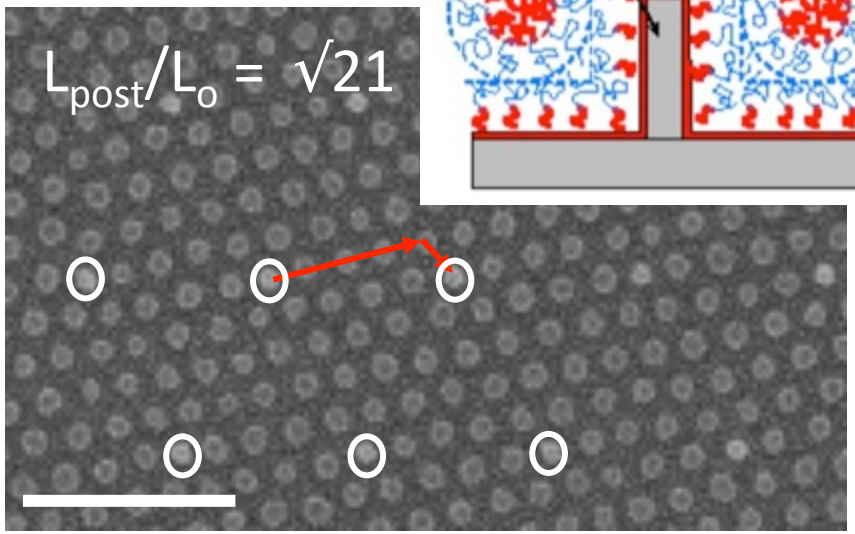

Bita et al, Science 321 939 (2008), Yang et al. Nature Nanotech. 5 256 (2010)

Monolayer of Cylinders

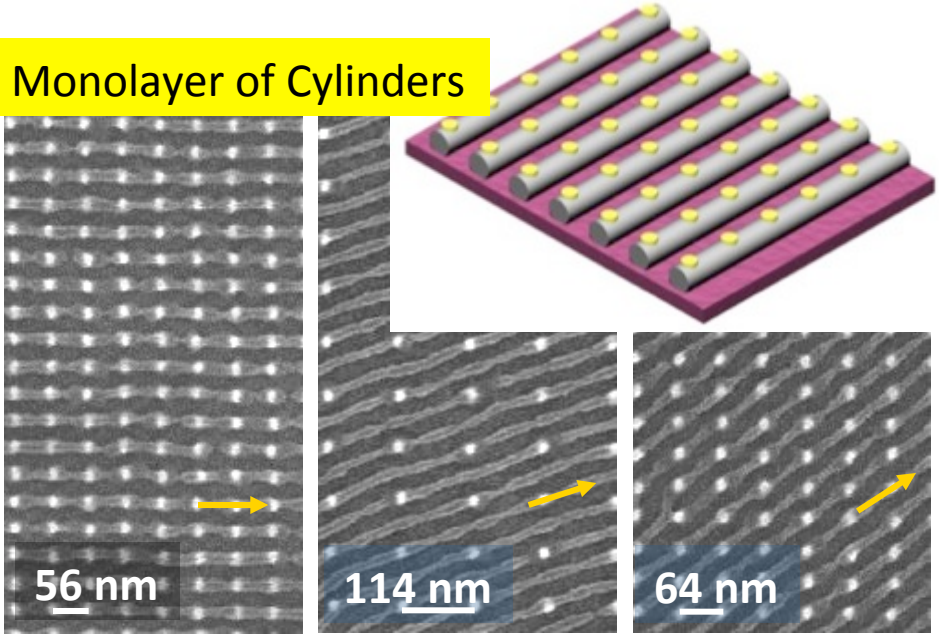

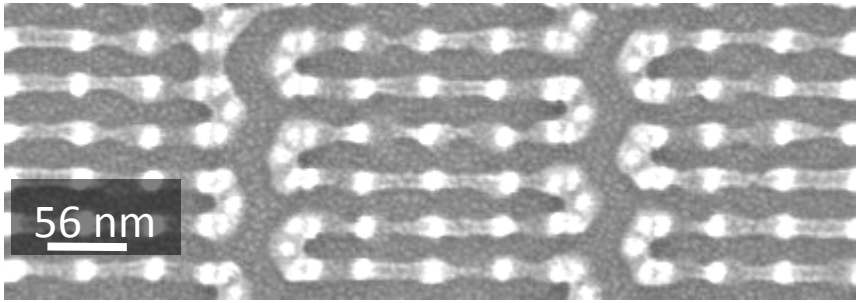

- Posts are attractive to PDMS block
- Commensurability governs pattern formation: The observed microdomain arrangement is the one that minimises strain

Directed self assembly of non-periodic patterns

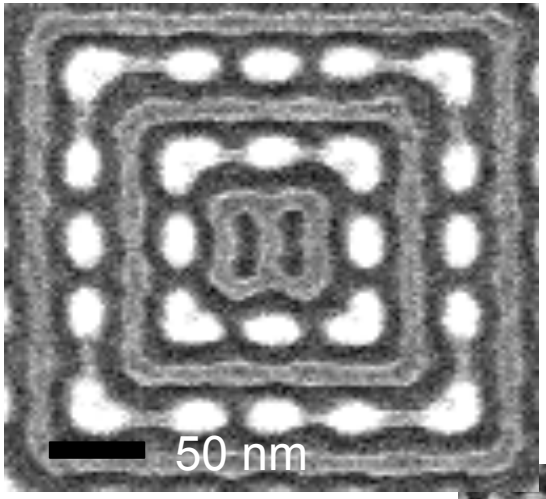

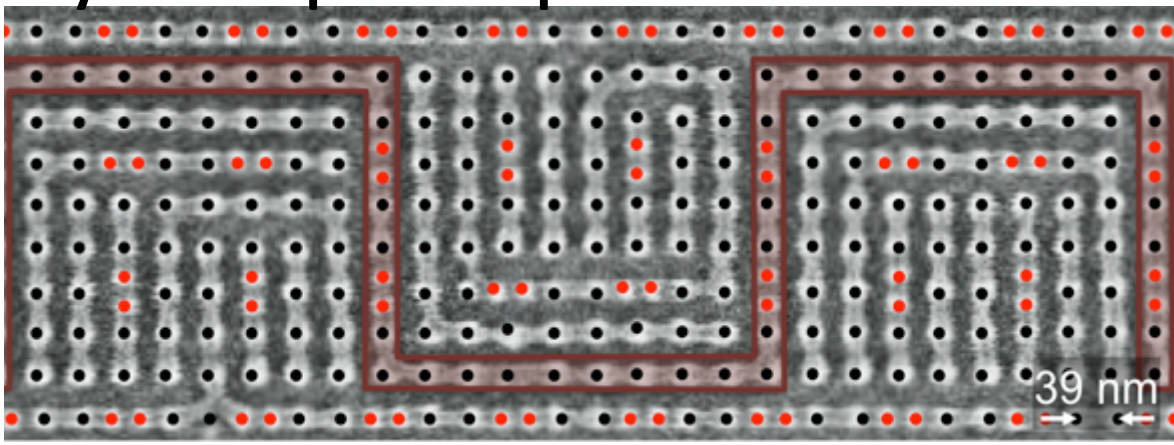

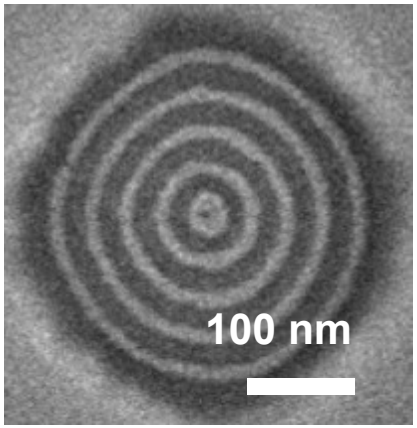

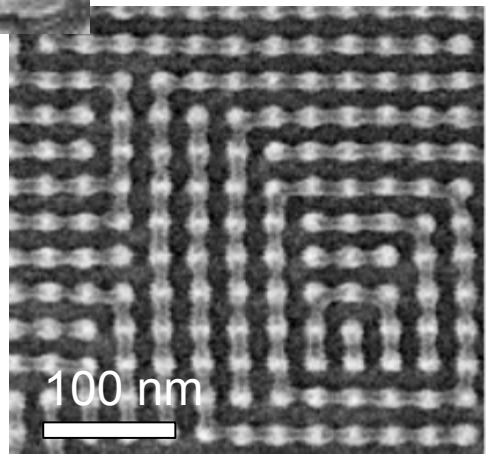

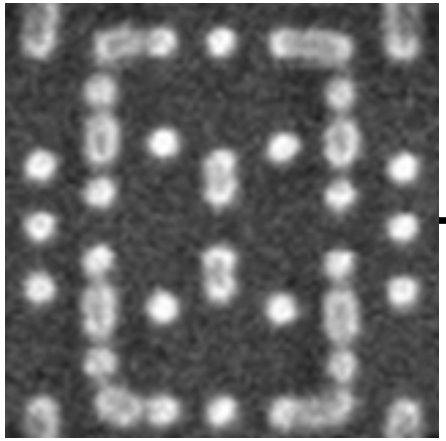

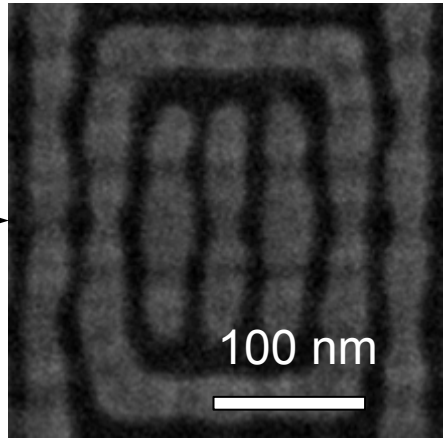

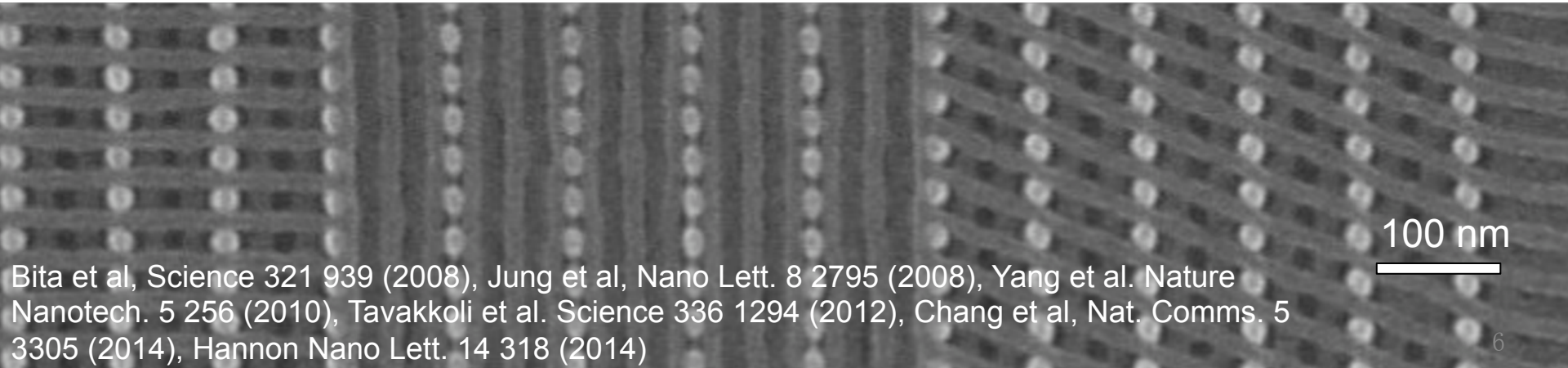

Bita et al, Science 321 939 (2008), Jung et al, Nano Lett. 8 2795 (2008), Yang et al. Nature Nanotech. 5 256 (2010), Tavakkoli et al. Science 336 1294 (2012), Chang et al, Nat. Comms. 5 3305 (2014), Hannon Nano Lett. 14 318 (2014)

Templating bilayers of cylinders

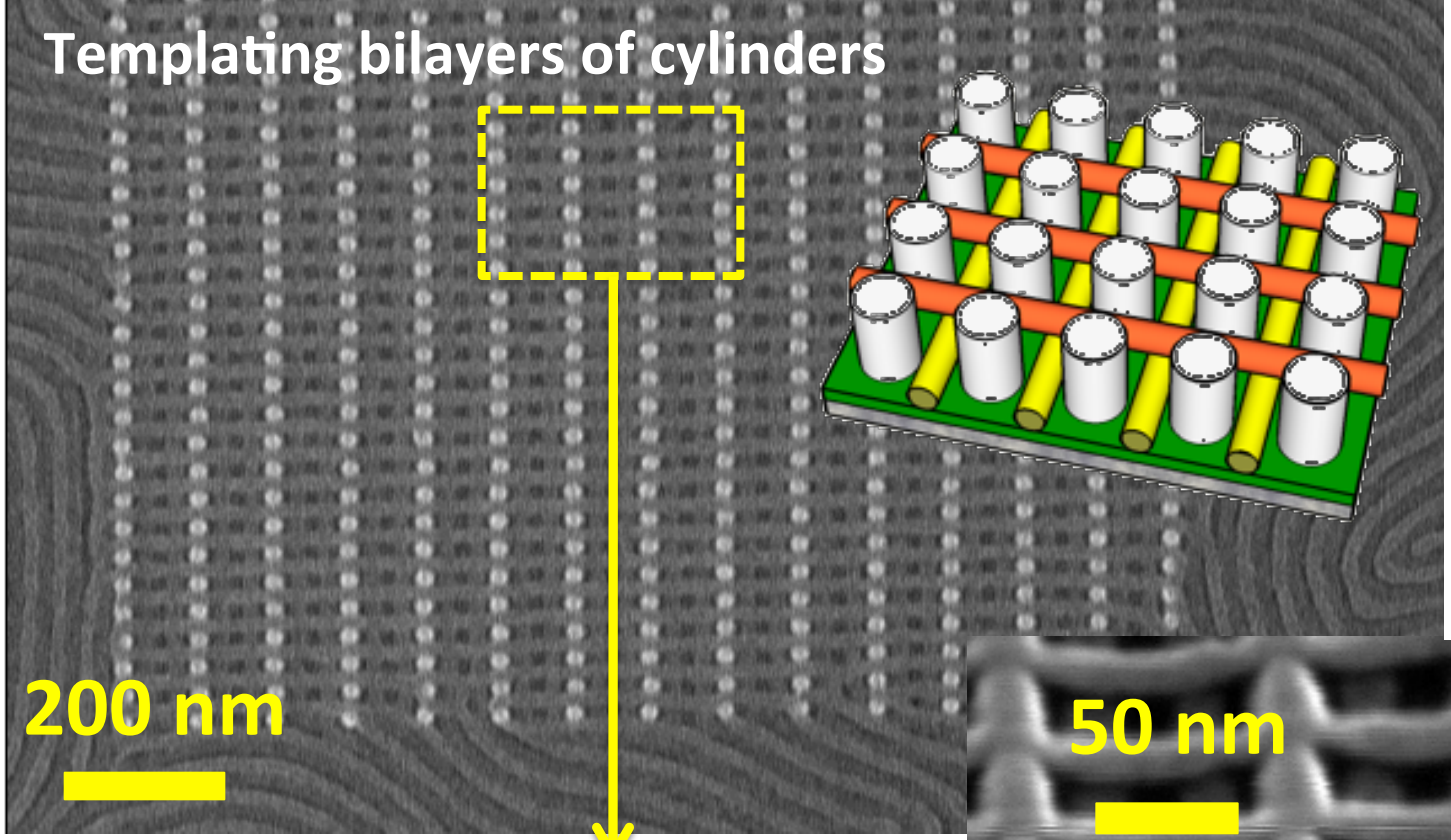

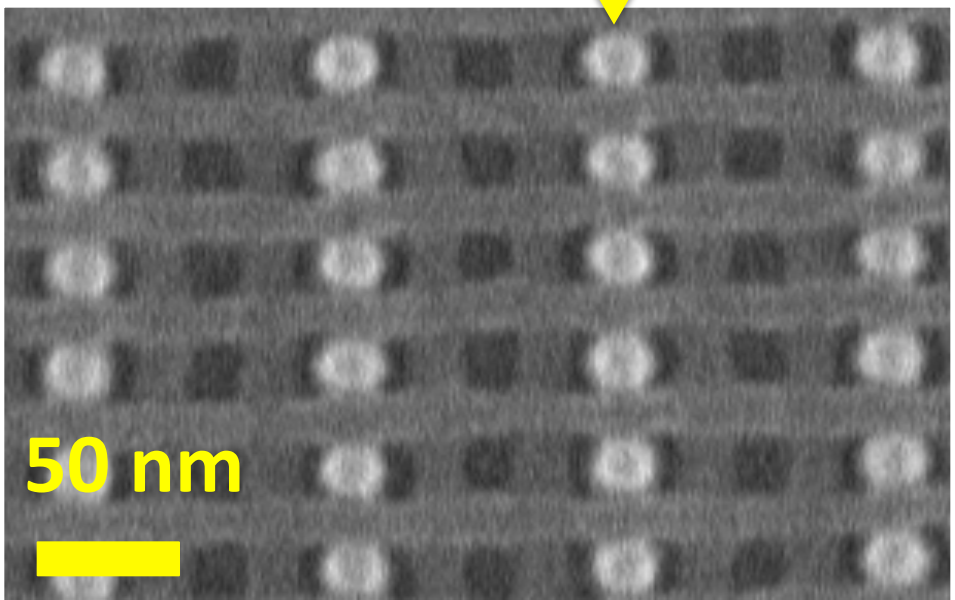

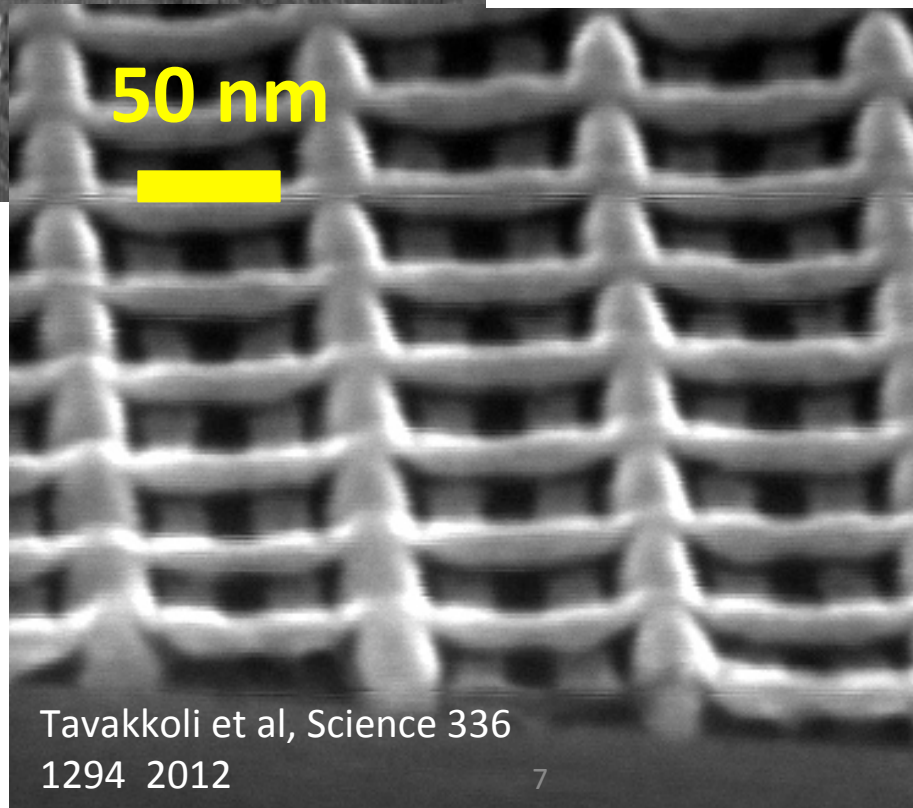

Tavakkoli et al, Science 336 1294 2012

Self assembly of one polymer on another

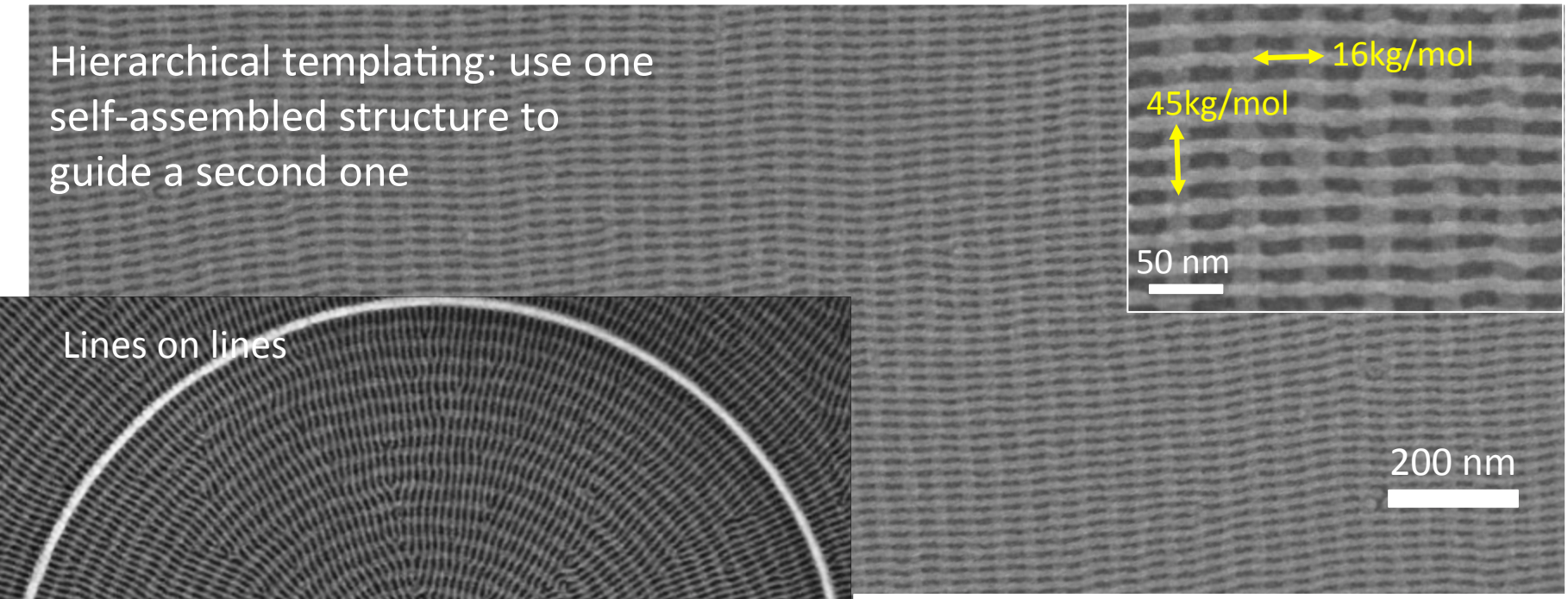

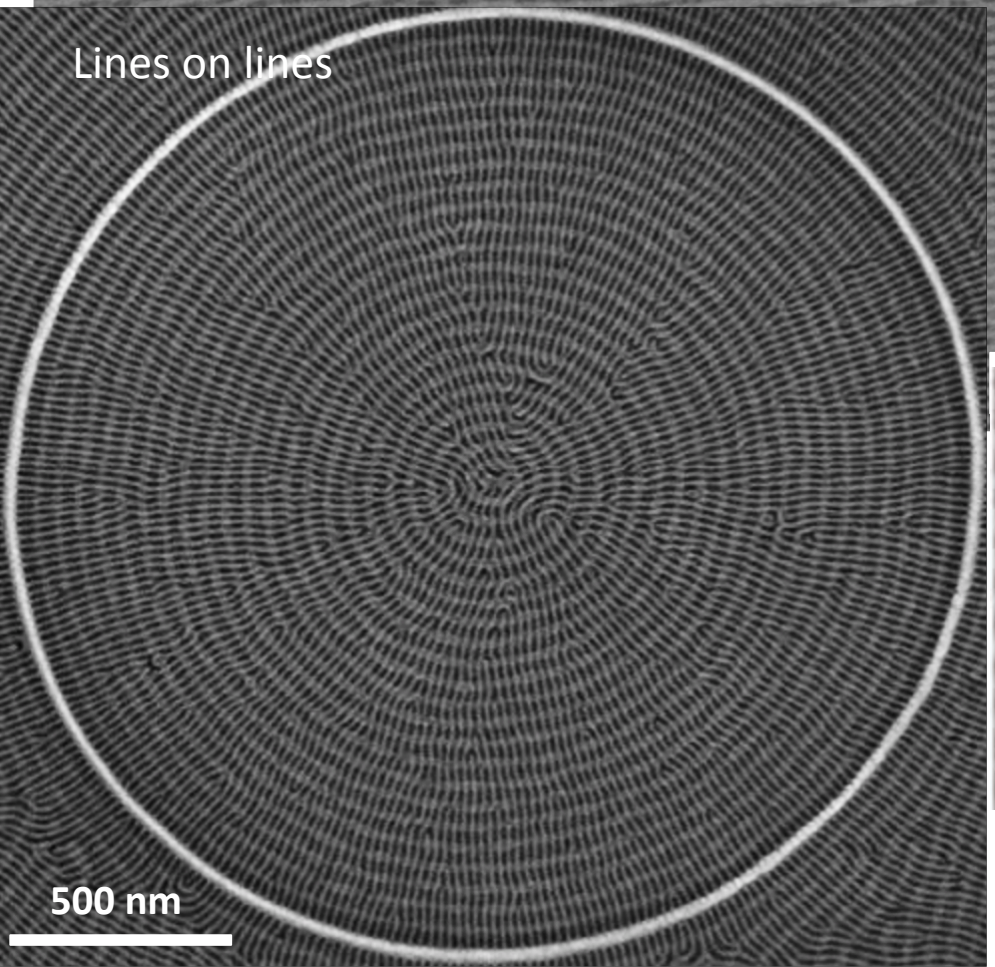

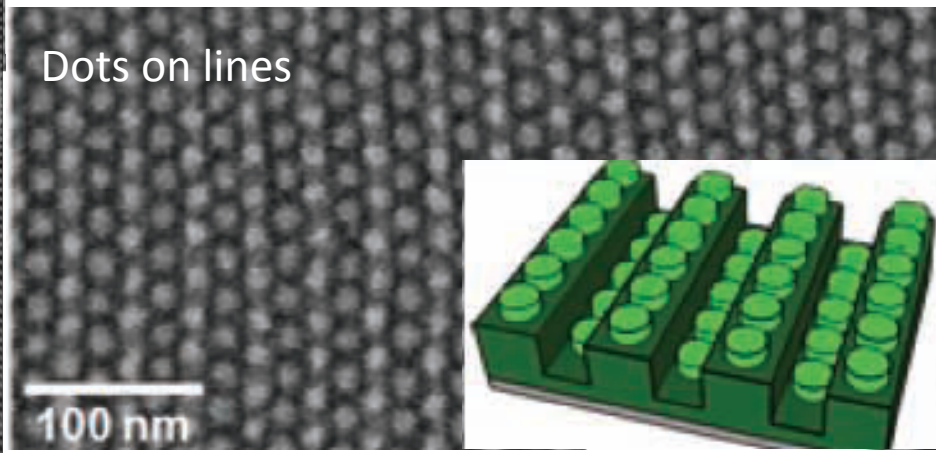

Tavakkoli et al, Nat. Comms. 7 10518 (2016);
Son et al, Adv. Mater. 23, 634 (2011)

Multiblock Copolymers

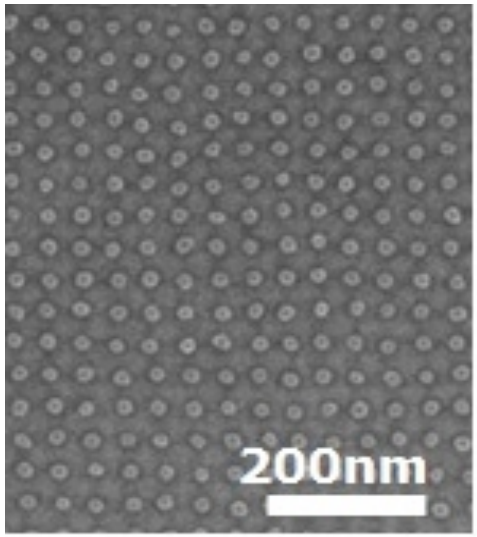

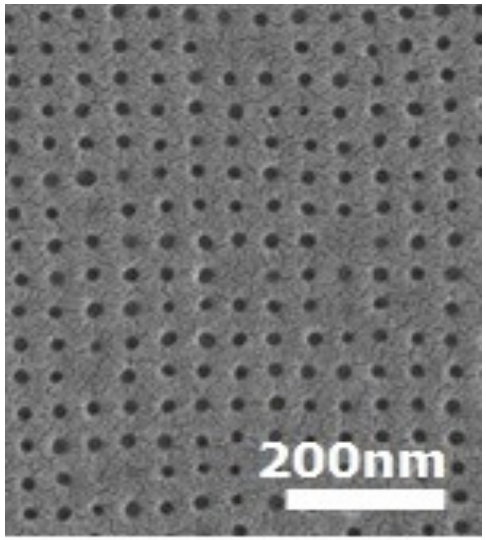

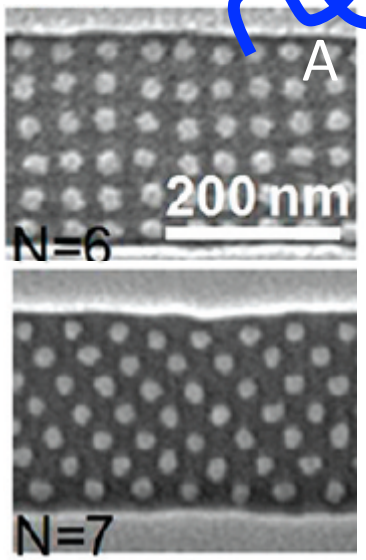

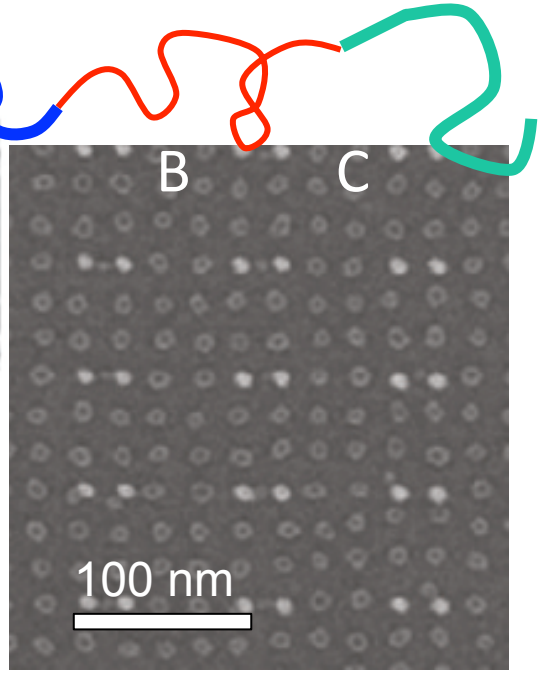

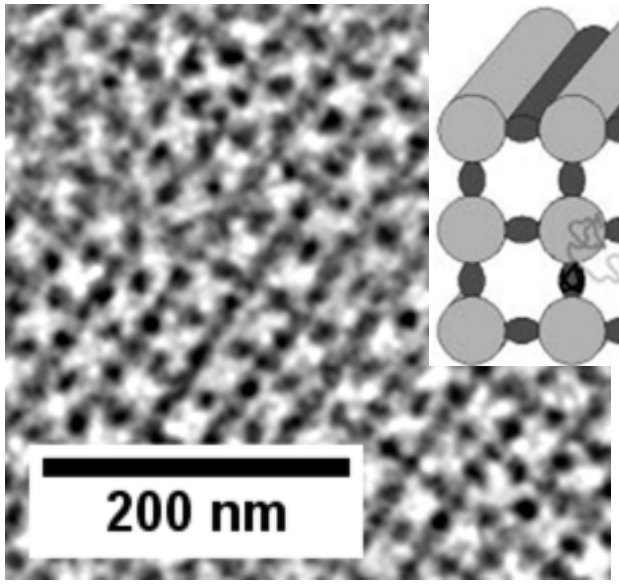

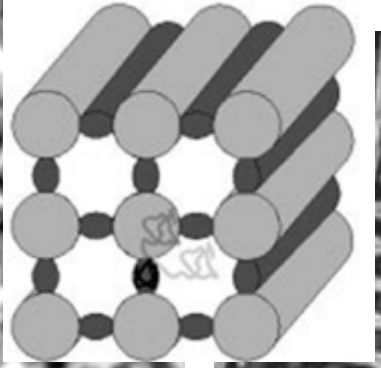

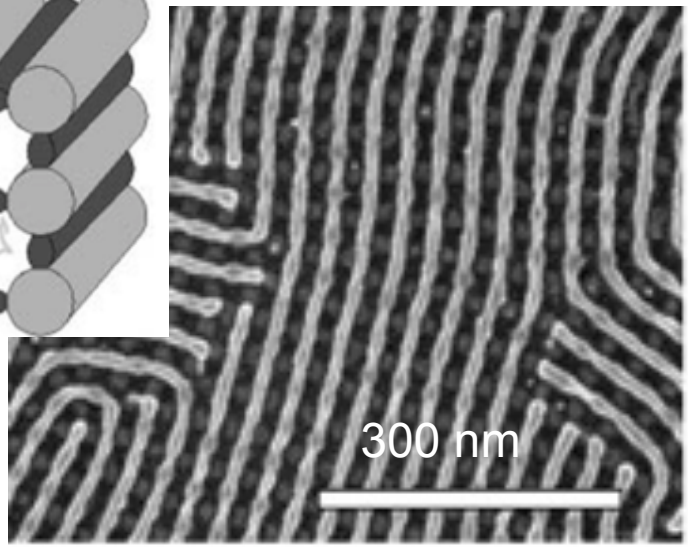

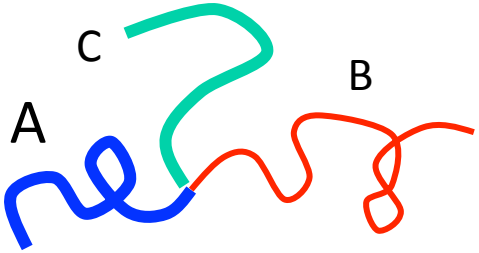

Chuang et al, N Letts 9 4364 (2009); Son et al, N Letts 11 2849 (2011); Choi et al, Adv. Mater. 26 2474 (2014); Aissou et al, Nano Lett 13 835 (2013)

- Archimedean tilings, square symmetry patterns, core-shell structures and other geometries are available from multiblock copolymers.

Block copolymer annealing processes

Thermal Annealing

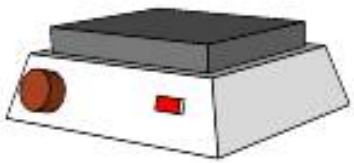

Solvent Annealing

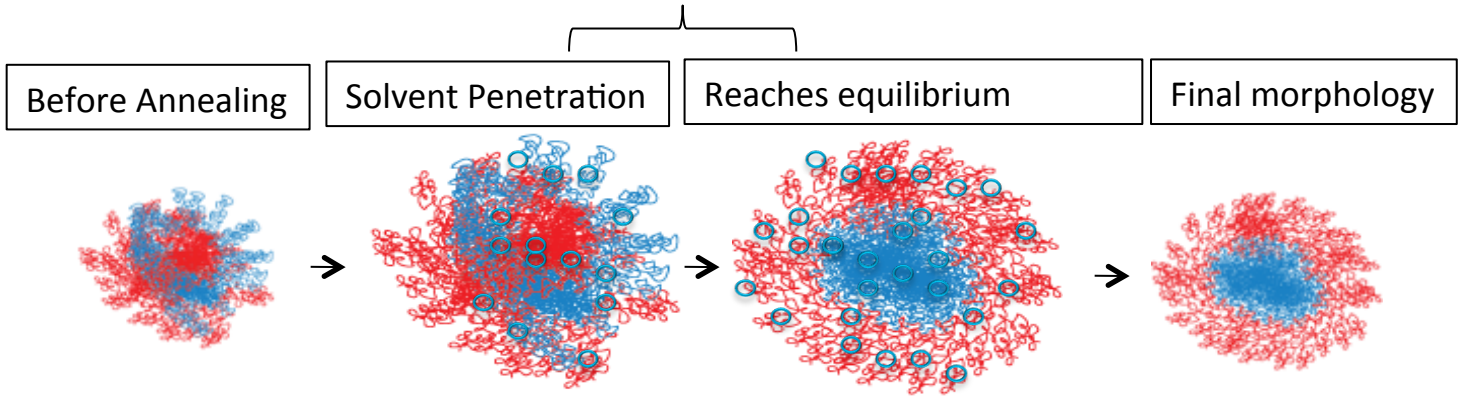

Thermal anneal:
-produces bulk morphology
-requires high T for high χN BCPs

Solvent anneal:
-improves BCP mobility
-decreases energetic barrier for diffusion
-produce non-bulk morphologies in selective solvents
-details poorly understood

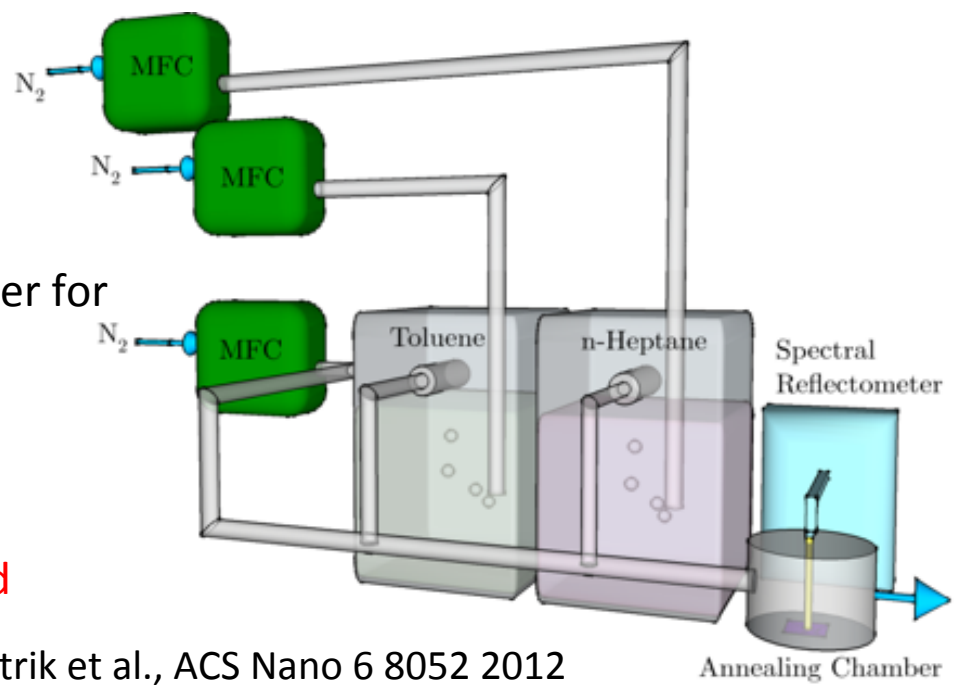

Gotrik et al., ACS Nano 6 8052 2012

PS-PDMS morphology tunability by solvent anneal

75 kg/mol , f_{PDMS} = 0.415 (bulk gyroid)

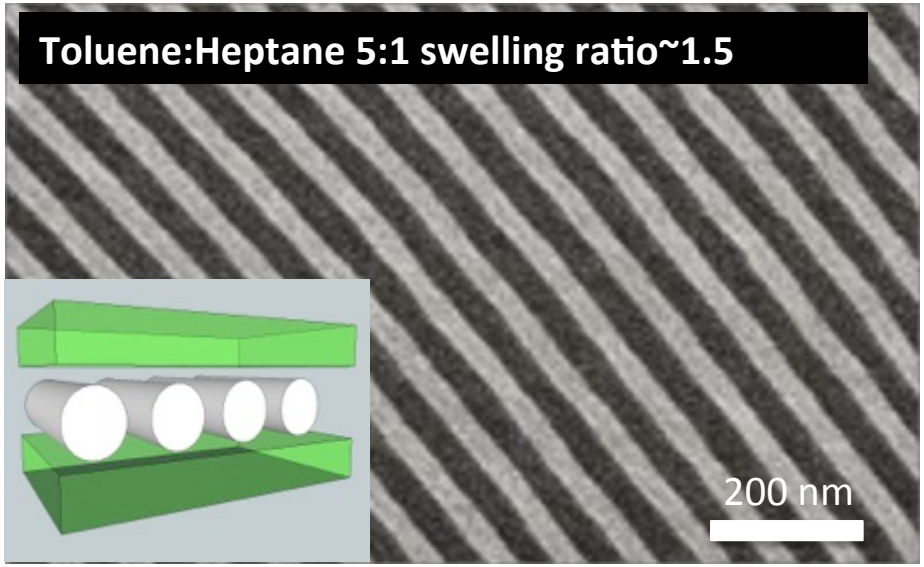

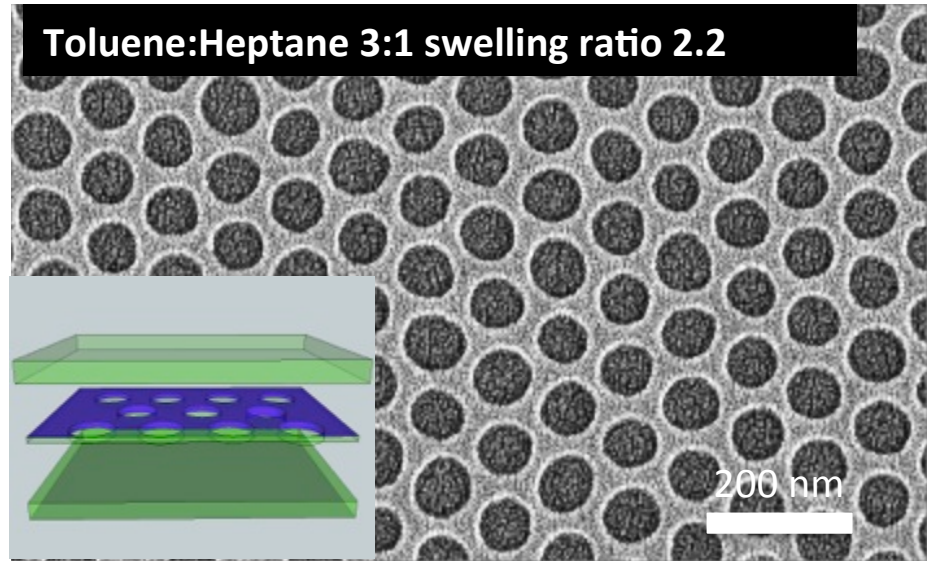

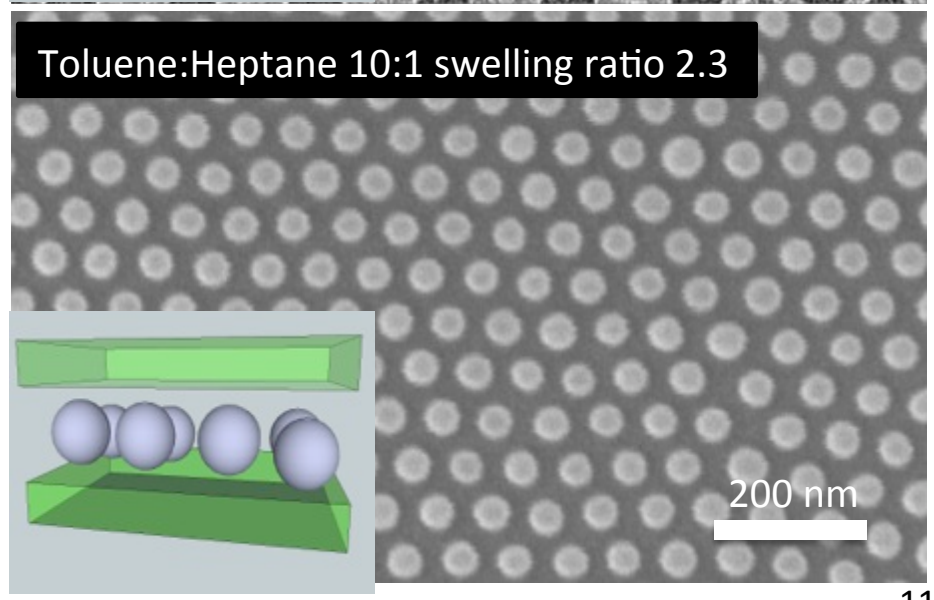

As-cast film thickness 45 nm

Toluene: Heptane (Swelling Ratio)	3:1 (2.2)	5:1 (1.5)	10:1 (2.5)
$p_{toluene}$(Torr)	10.37	7.86	14.29
$p_{heptane}$(Torr)	6.29	2.86	2.60

Specific thickness and solvent anneal gives well ordered, tunable, non-bulk structures

Bai et al., Macromol. 47 6000 (2014)

Orientation control by solvent anneal

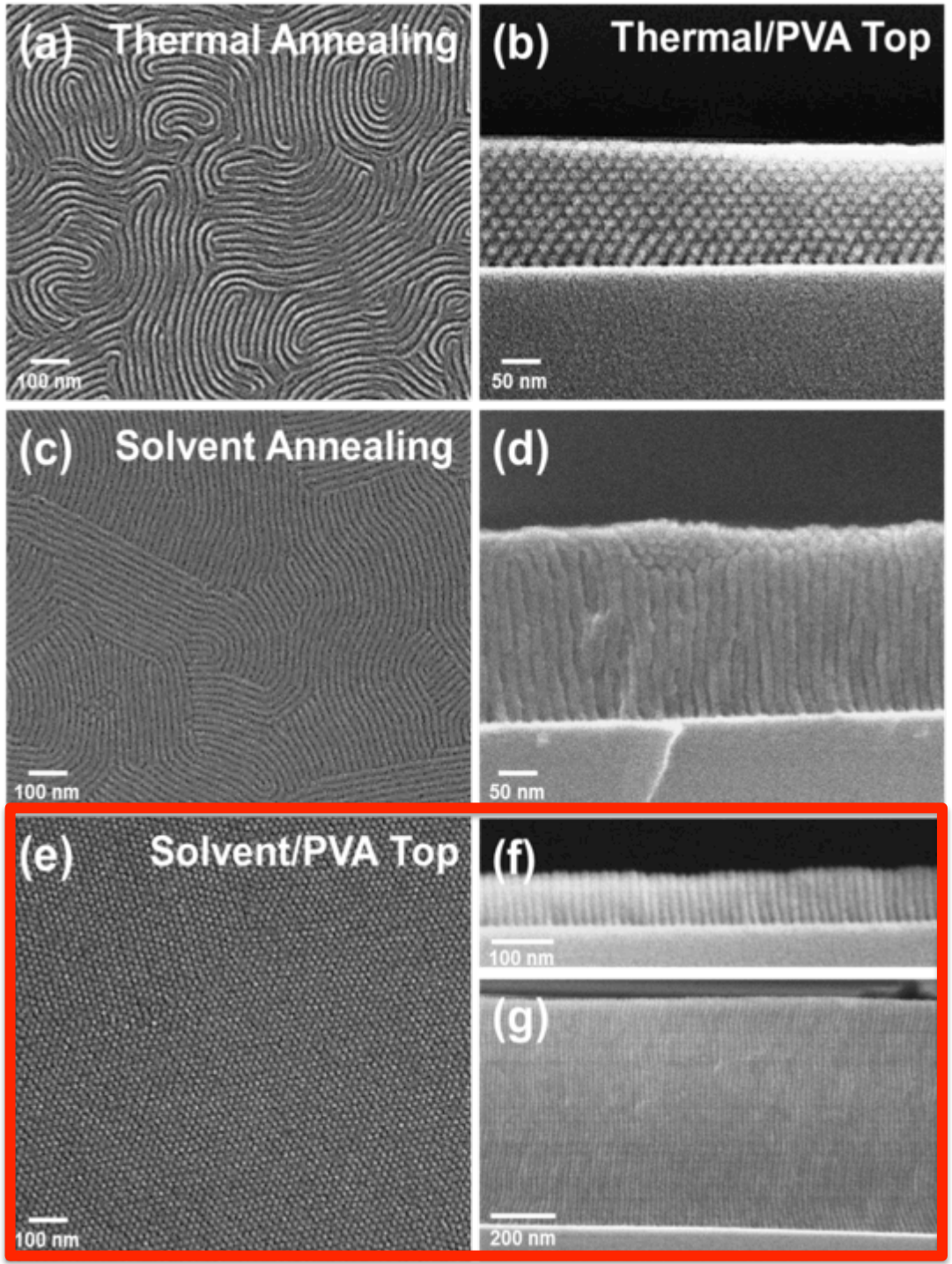

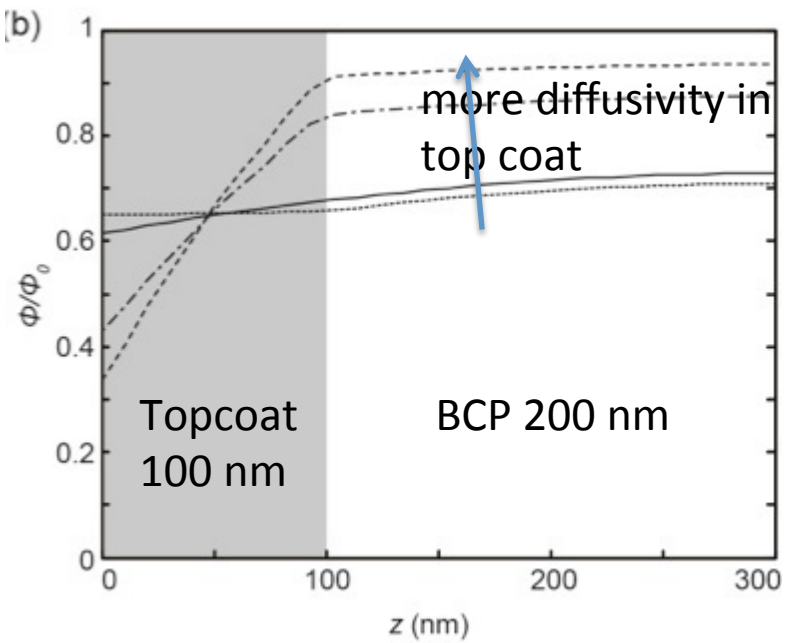

Solvent gradient in film

Fully perpendicular cylinders in high-χ block copolymer using slow drying and topcoat

Son et al., Adv. Fn. Mater. 24 6981 (2014)

Demystifying Solvent anneal: Evolution of 3D Structures

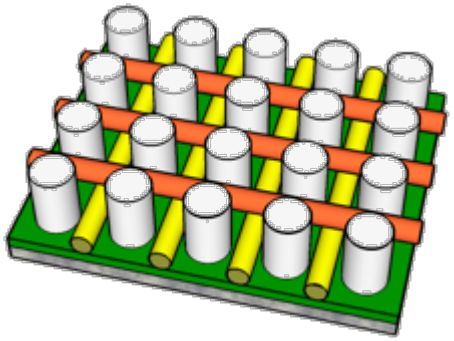

As-cast film

swell, heat

Structure of swollen film during solvent anneal

In-situ grazing incidence Xray scattering

deswell, cool

Structure of unetched film after deswelling

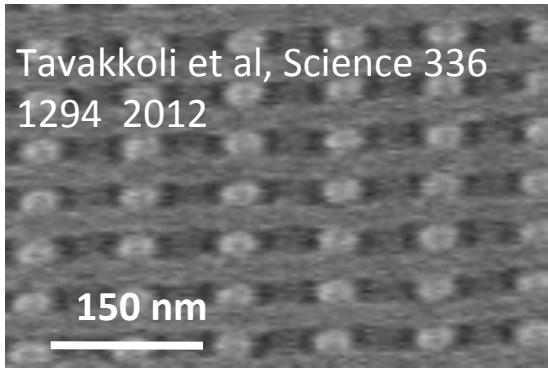

Tavakkoli et al, Science 336 1294 2012

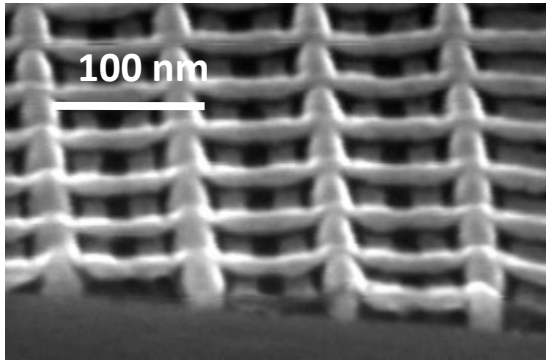

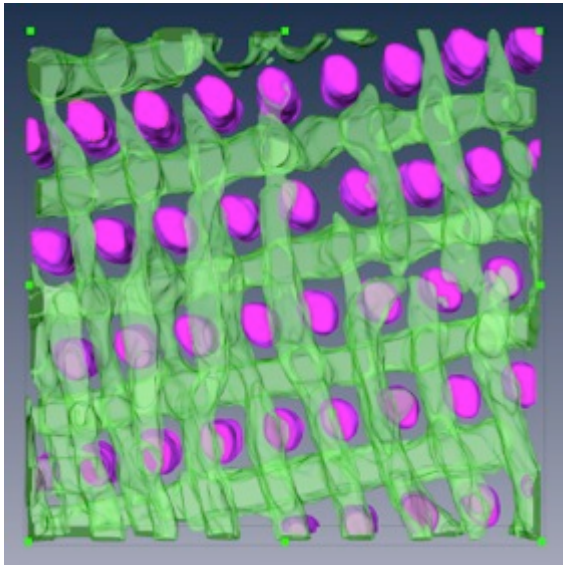

TEM tomography of unetched film

Final structure of the remaining block of the BCP on wafer

TEM or SEM

TEM Tomography of unetched film

NIST (Thomas Lam, Alex Liddle)

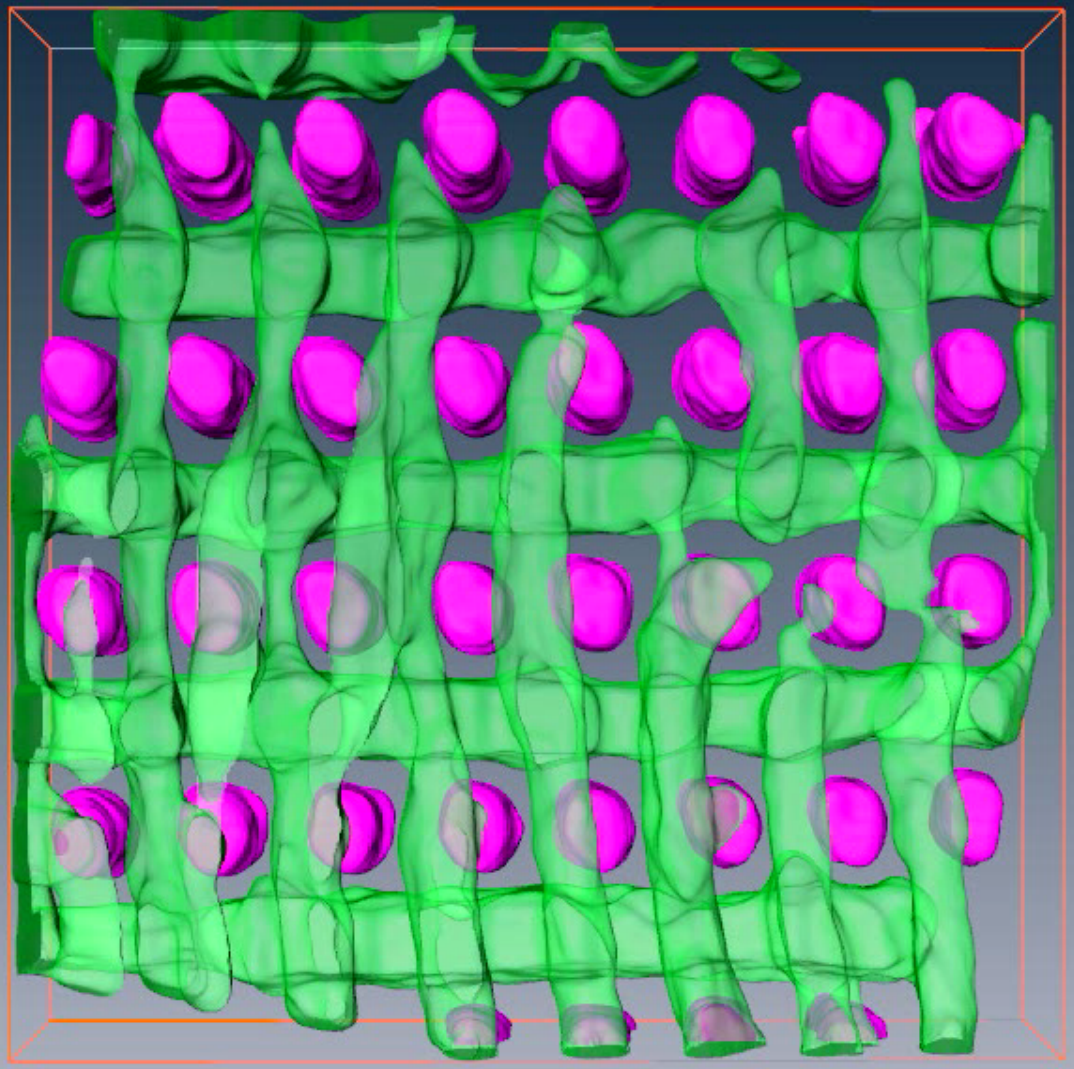

Gotrik, Lam et al., Adv. Funct. Mater. 24 7689 (2014)

295 nm by 295 nm
41 nm thick
Voxel = 0.85 nm

Cylinders are connected at cross-points

Microdomain evolution in the swelled state by GISAXS

PS-PDMS, 16kg/mol, 5:1 toluene:heptane
As-cast film thickness 230 nm
Measured at Brookhaven, K. Yager/W. Bai

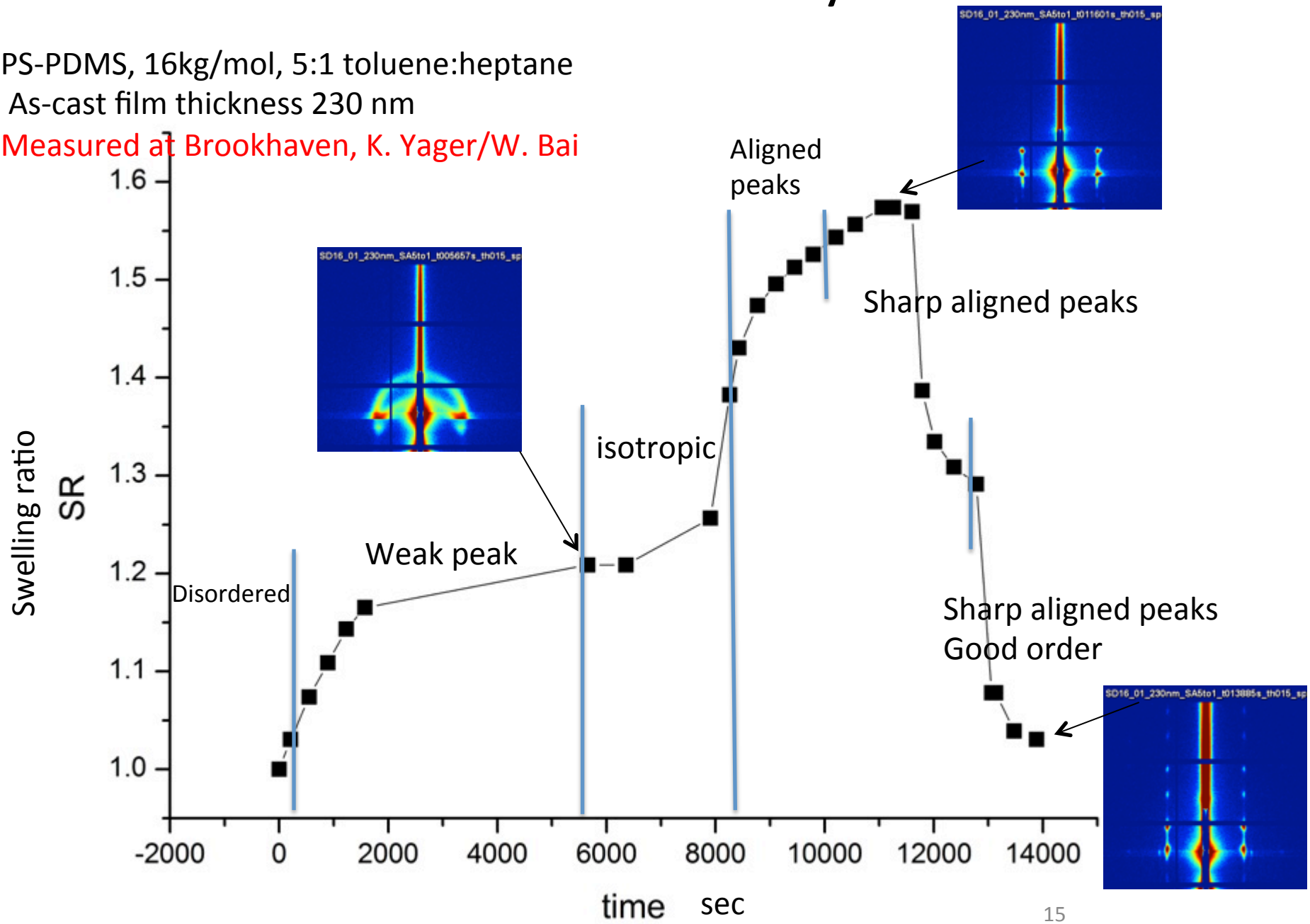

Microdomain evolution in the swelled state by GISAXS

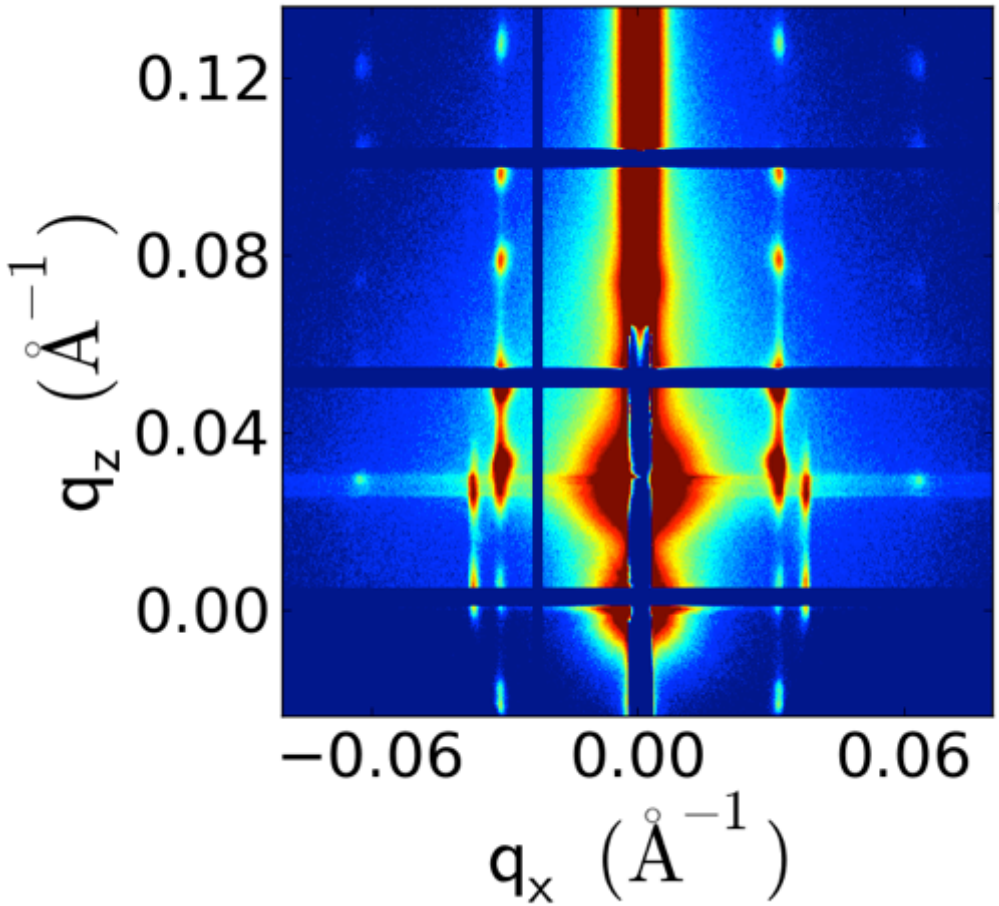

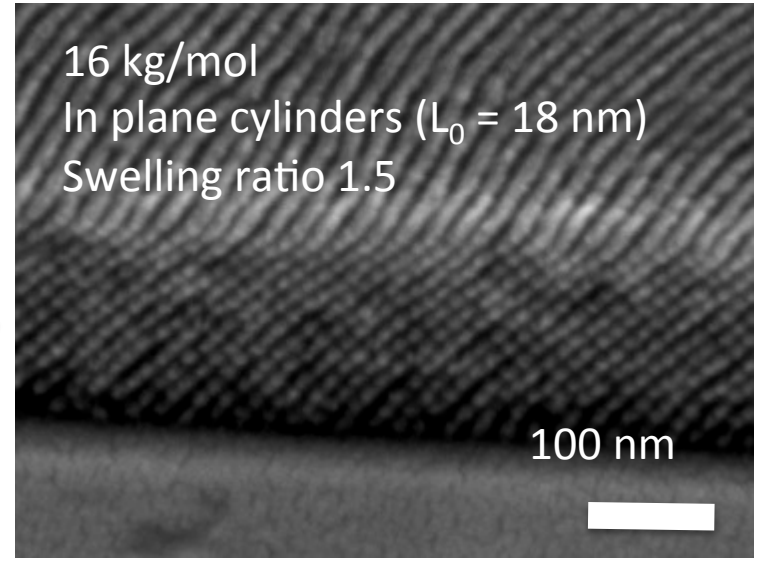

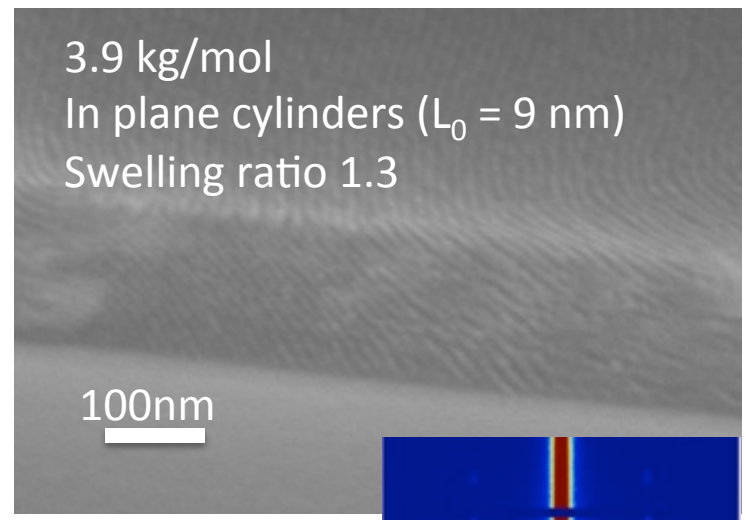

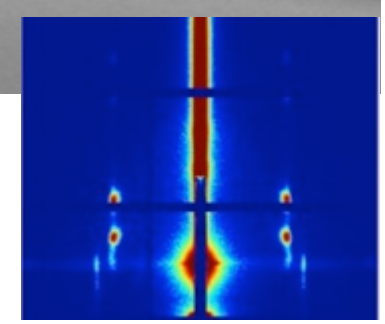

- Maximum swelling ratio, time in swelled state, deswelling rate all affect morphology
- Thicker films have more out-of-plane cylinders
- More heptane produces cylinder-> lamellar transition
- Even 3.9 kg/mol PS-PDMS shows microphase separation (period <10 nm)

Orientation of Cylinders in Thin and Thick Films

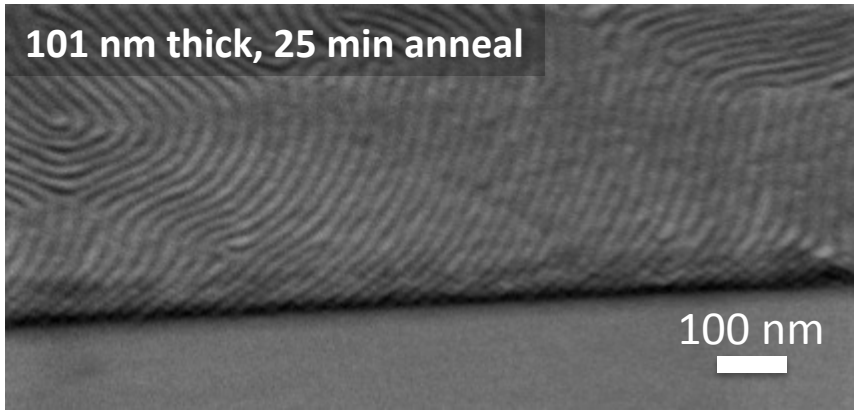

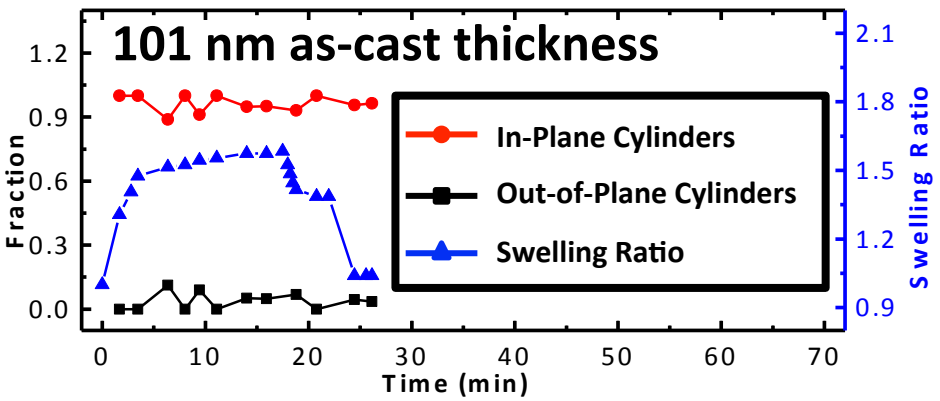

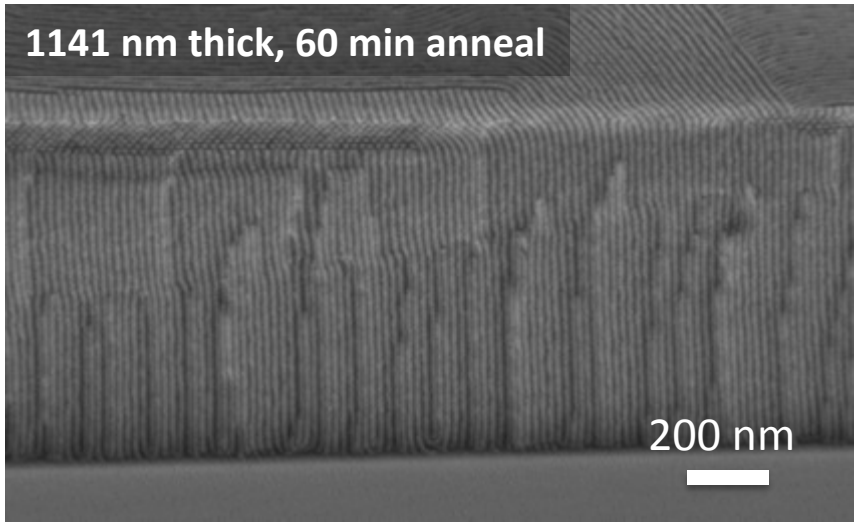

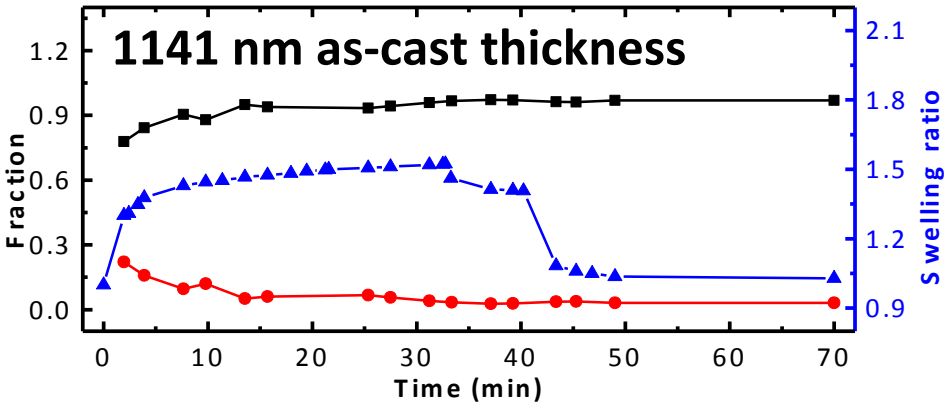

Thin Film, Strong Surface interaction induces In-Plane Orientation

Thick Film, solvent concentration gradient facilitates Out-of-Plane Orientation

W. Bai, K. G. Yager, C. A. Ross, Macromolecules 48 8574 (2015), Polymer 101 176 (2016)

Orientation of Cylinders in Intermediate Films

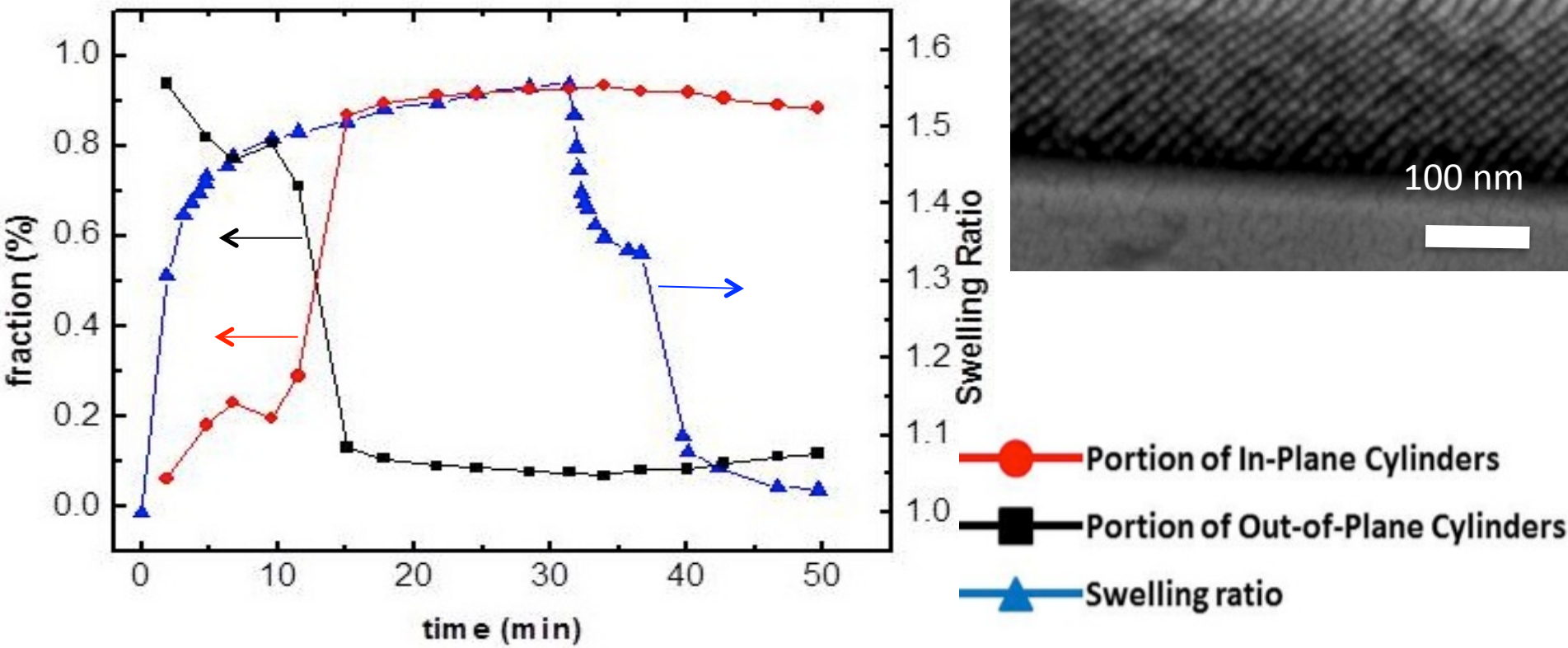

- Early stage of anneal: **Cylinders out-of-plane** due to solvent conc. gradient
- **Reorientation to in-plane** driven by surface interactions
- In-plane orientation dominates for thinner films

W. Bai, K. G. Yager, C. A. Ross, Macromolecules 48 8574 (2015), Polymer 101 176 (2016)

Collapse of structure during drying

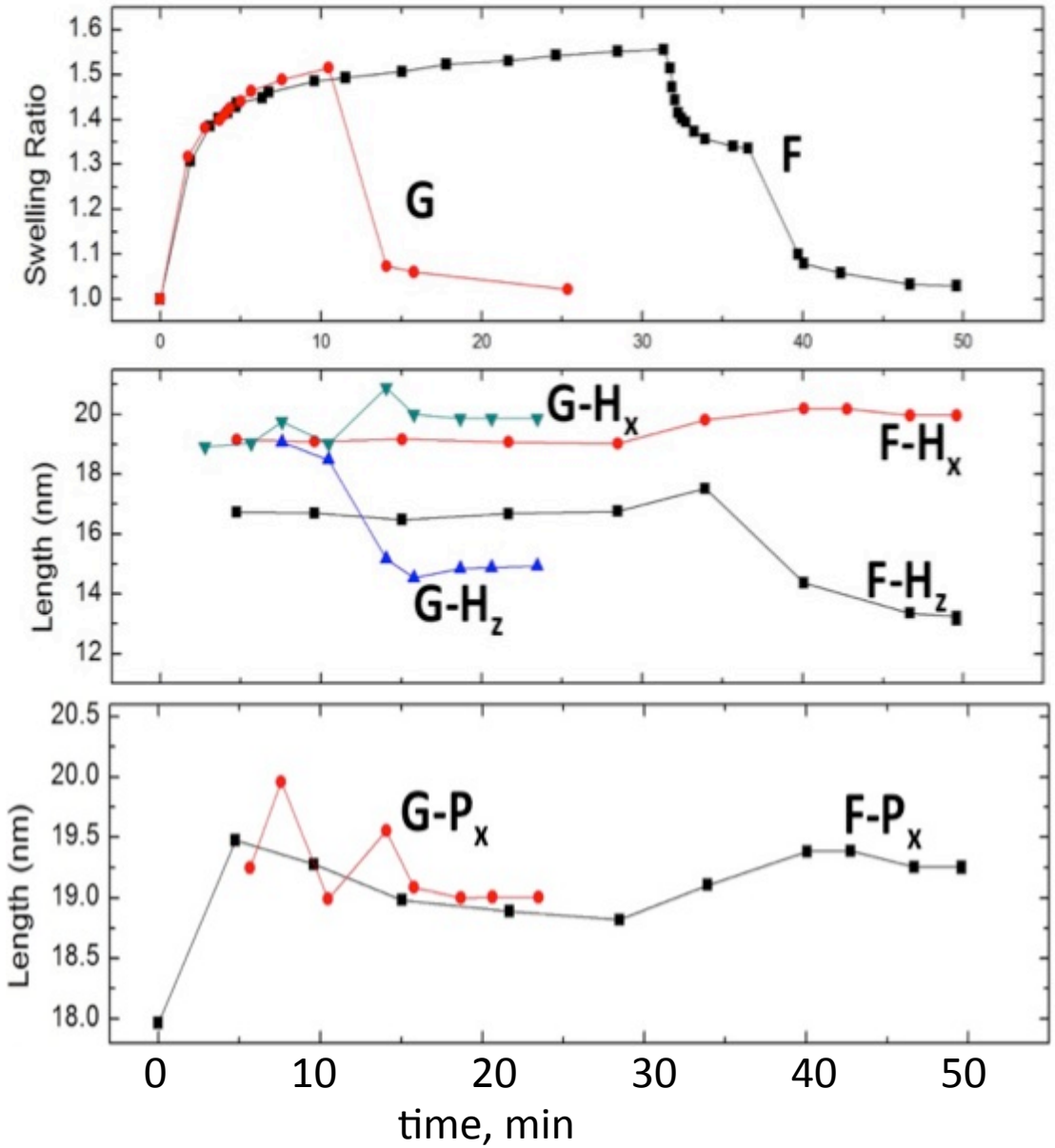

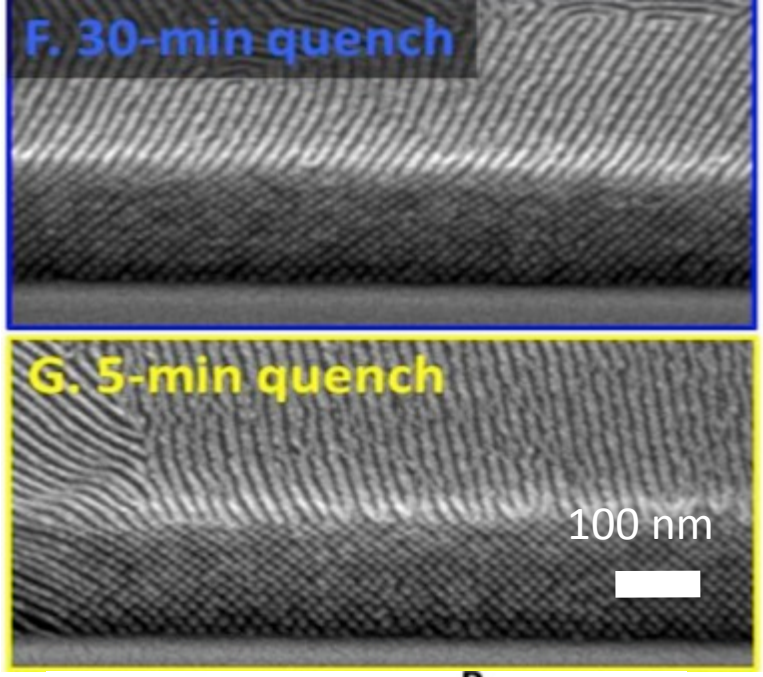

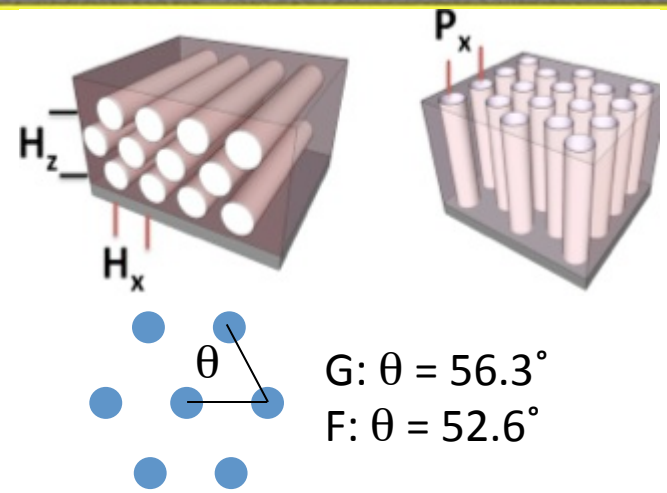

- On quenching, structure **collapses in OP direction**
- Little change in IP period
- Distortion fn. of anneal process

Incorporation of functional nanoparticles in block copolymer

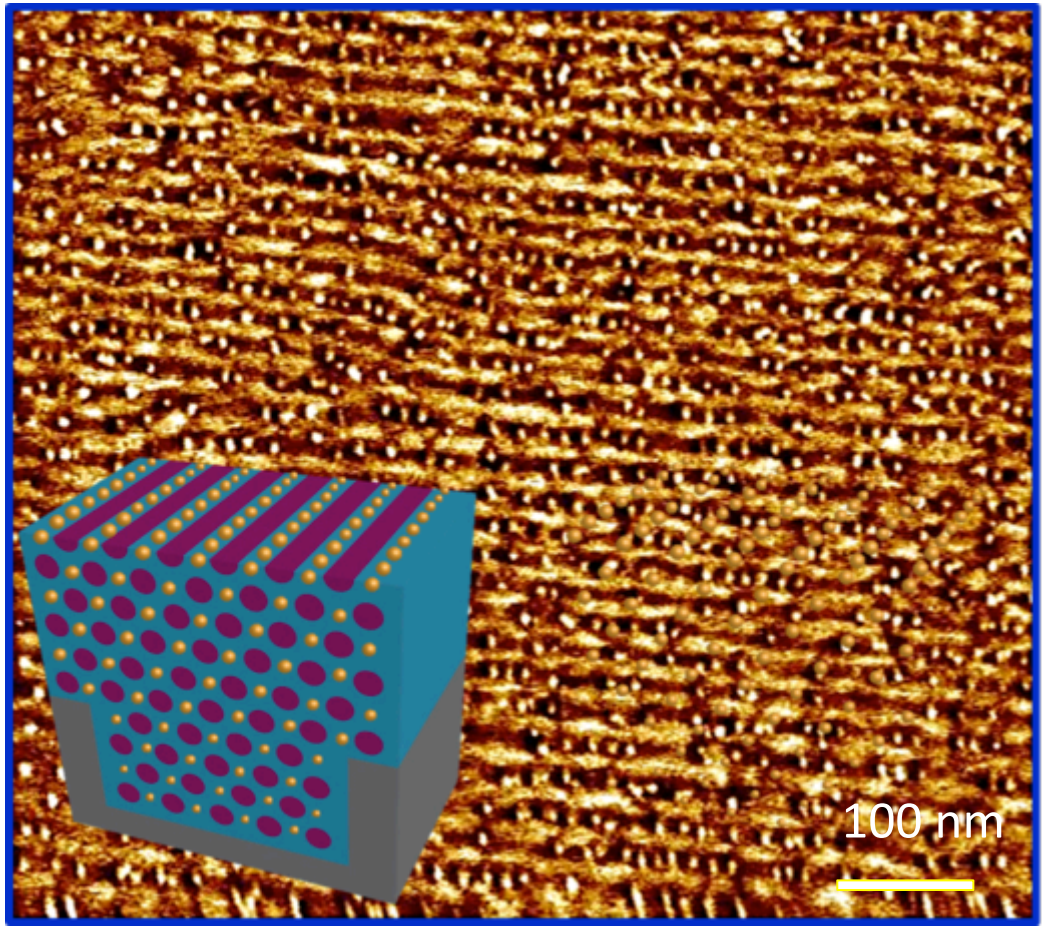

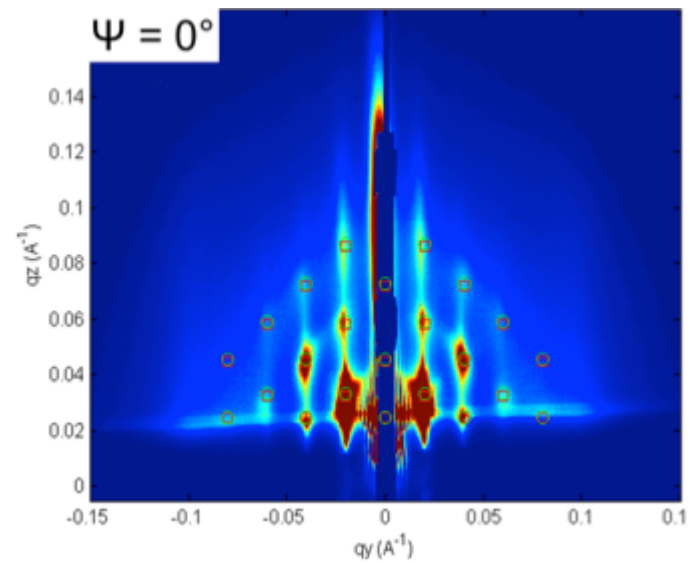

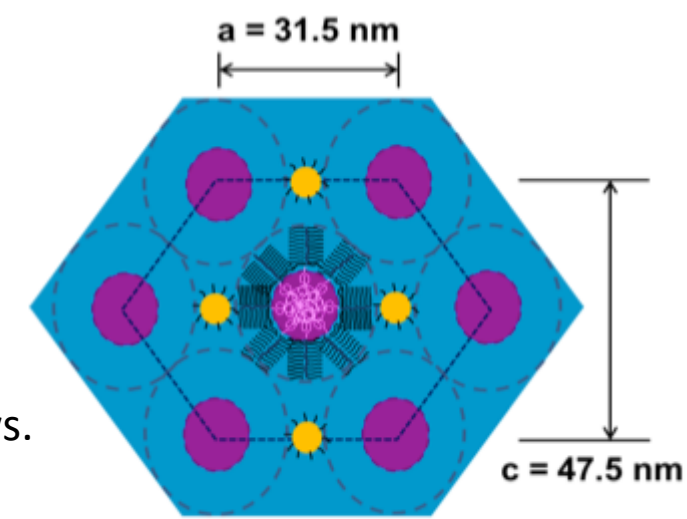

On lithographic trench pattern
(L = 125 nm)

Thick film (>10 layers) of cylindrical block copolymer.
Au nanoparticles arranged between cylinders to form rows.
Overall alignment templated by trenches.

PS(19 kDa)-*b*-P4VP-(5.2 kDa) (PDI = 1.09) and 3-n-Pentadecylphenol with Au NPs in P4VP-PDP matrix

Kao et al, Adv. Mater. 26 2777 **2014**

New directions

- **Bottle brush block copolymers** – kinetics of annealing
- **Triblock terpolymers** – Sequence of steps during microphase separation: does A separate from B+C
- **Liquid crystal block copolymers** – orientation of LC with respect to the coil microdomains

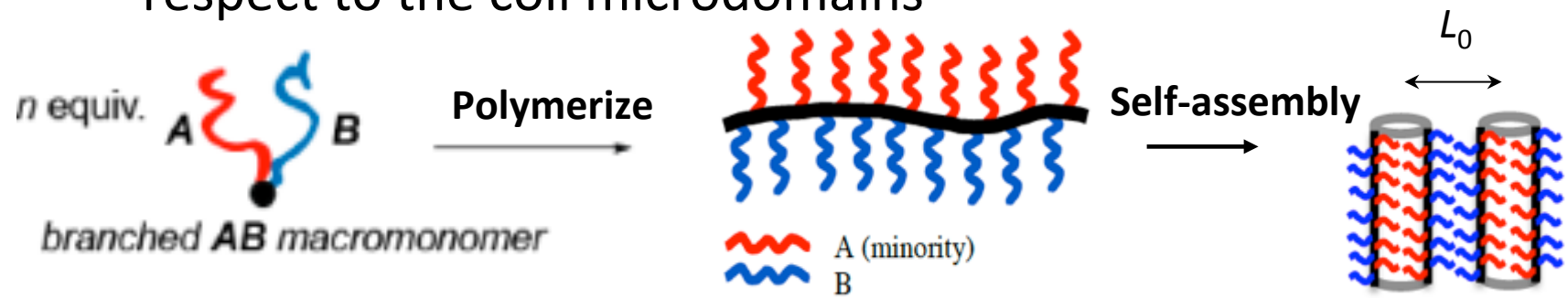

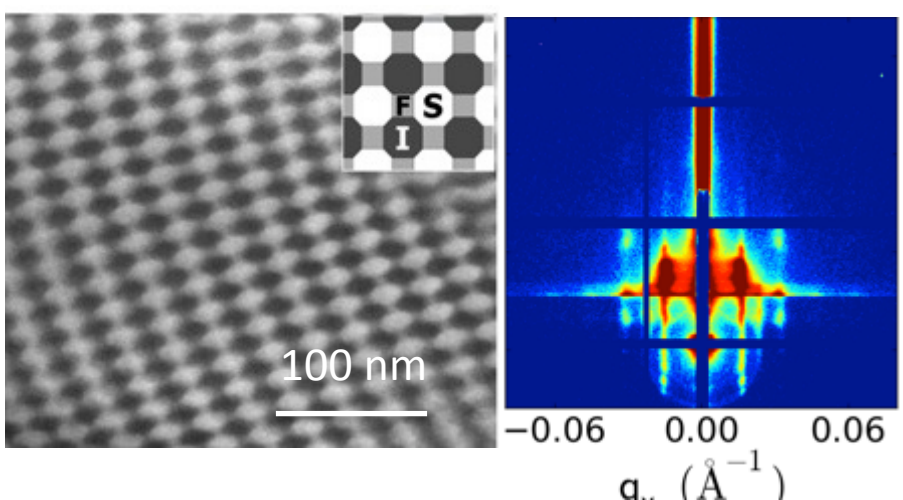

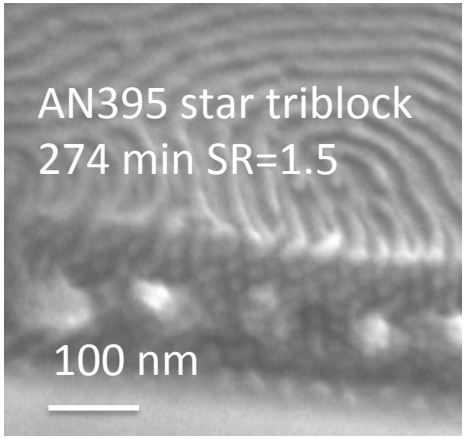

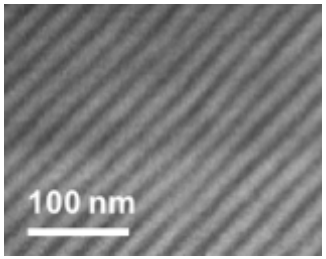

$(PS15.3k\text{-}br\text{-}PDMS5k)_{30}$
600 kg/mol, L_0 = 20 nm
Kawamoto et al, JACS 138 11501 (2016)

Magnetic Oxides – Garnets

- **$Y_3Fe_5O_{12}$ (YIG):** Ferrimagnetic insulator with very low magnetic damping.
- A cubic crystal with a =1.2 nm. Excellent lattice match with GGG ($Gd_3Ga_5O_{12}$).
- $3Fe^{3+}$ on tetrahedral and $2Fe^{3+}$ on octahedral sites are coupled antiferromagnetically; $5\mu_B$ per YIG.
- Replace Y with Bi, Ce, or rare earth to modify properties. RE magnetic moment is parallel to octahedral sites.

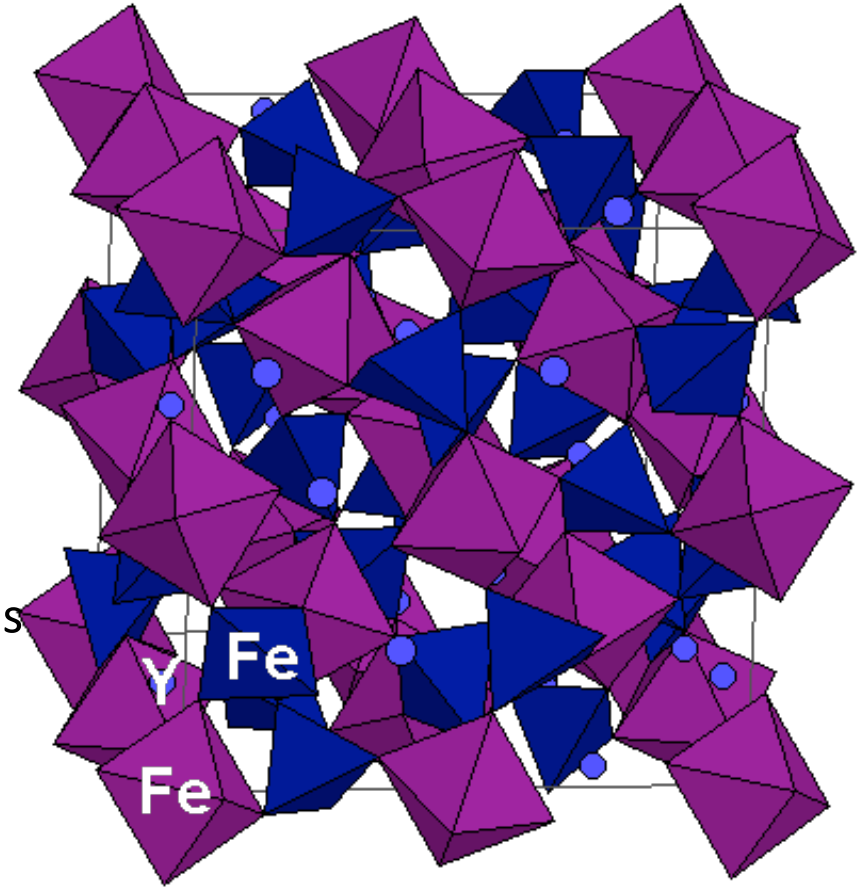

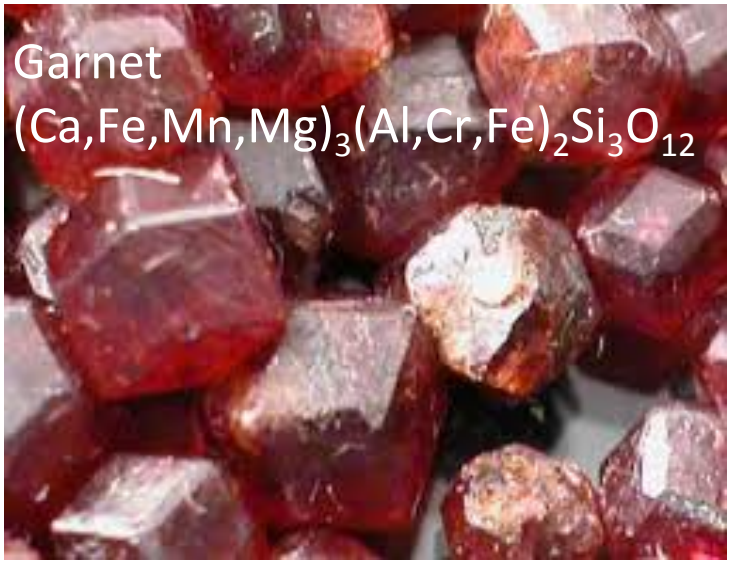

Interest in:

- spin wave propagation/magnetization dynamics
- heterostructures with topological insulators or heavy metals – spin mixing and pumping
- spin orbit torques
- bubbles, skyrmions and other textures

Garnets with perpendicular magnetic anisotropy

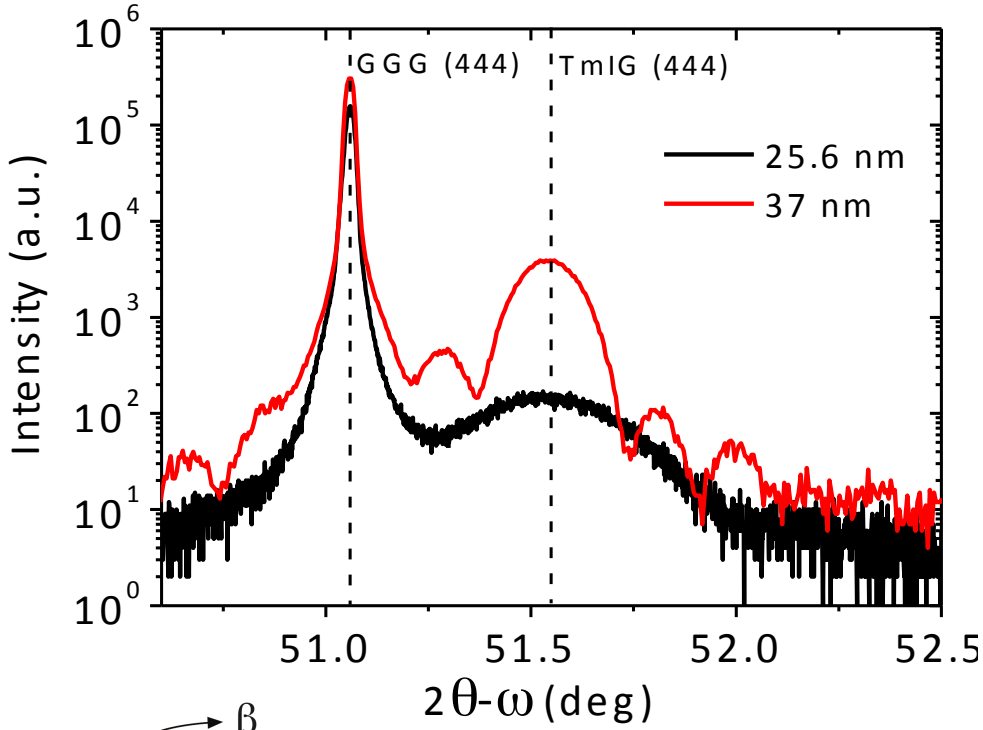

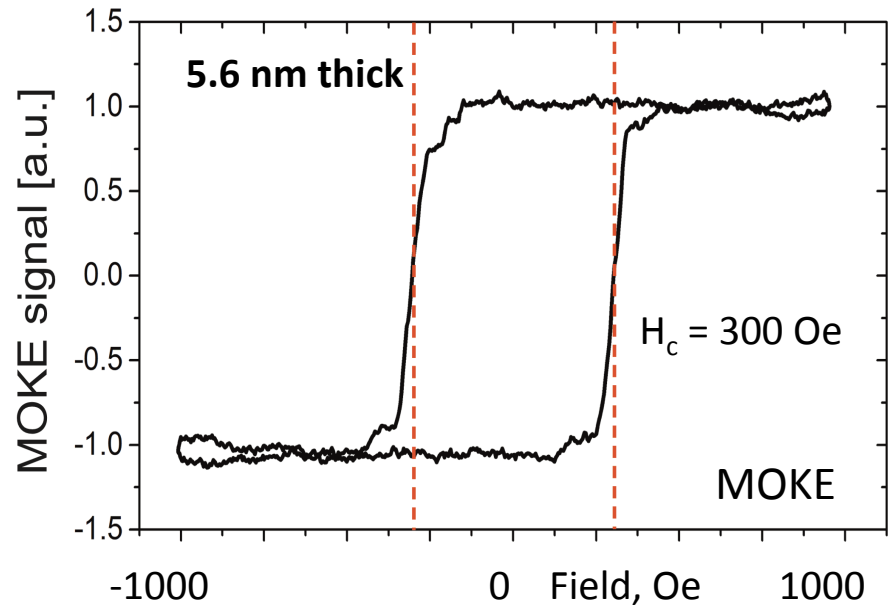

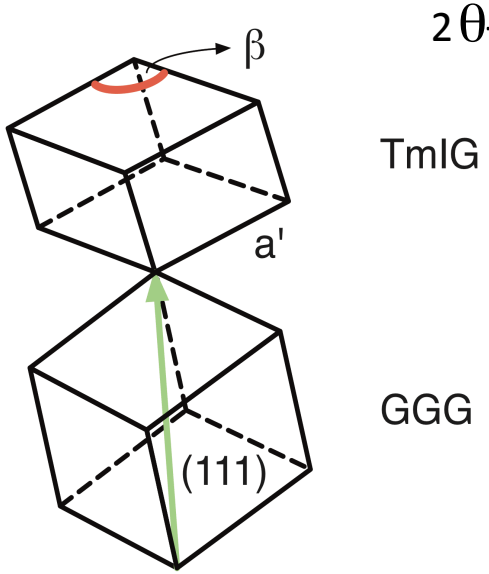

- YIG magnetization lies in plane. However,
- **$Tm_3Fe_5O_{12}$ (TmIG)**: (111) film has in-plane tension, negative magnetostriction combined with negative K_1 gives **OP easy axis**, overcoming shape anisotropy.
- β = 90.76˚ at room temperature

Quindeau et al, Adv. Electronic Mater. 1 1600376 (2017)

HRTEM of TmIG/GGG

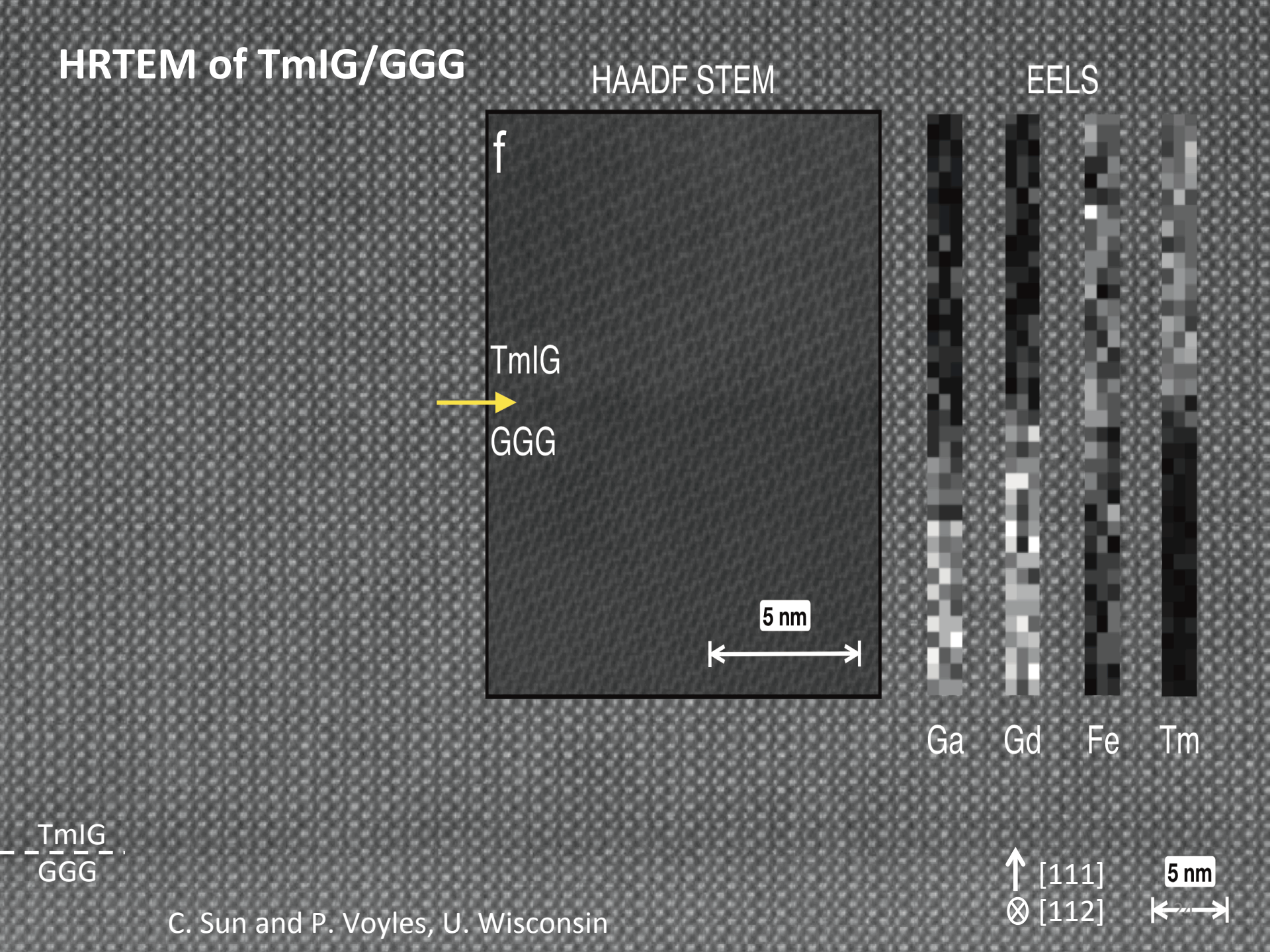

C. Sun and P. Voyles, U. Wisconsin

XMCD measurements of TmIG/GGG

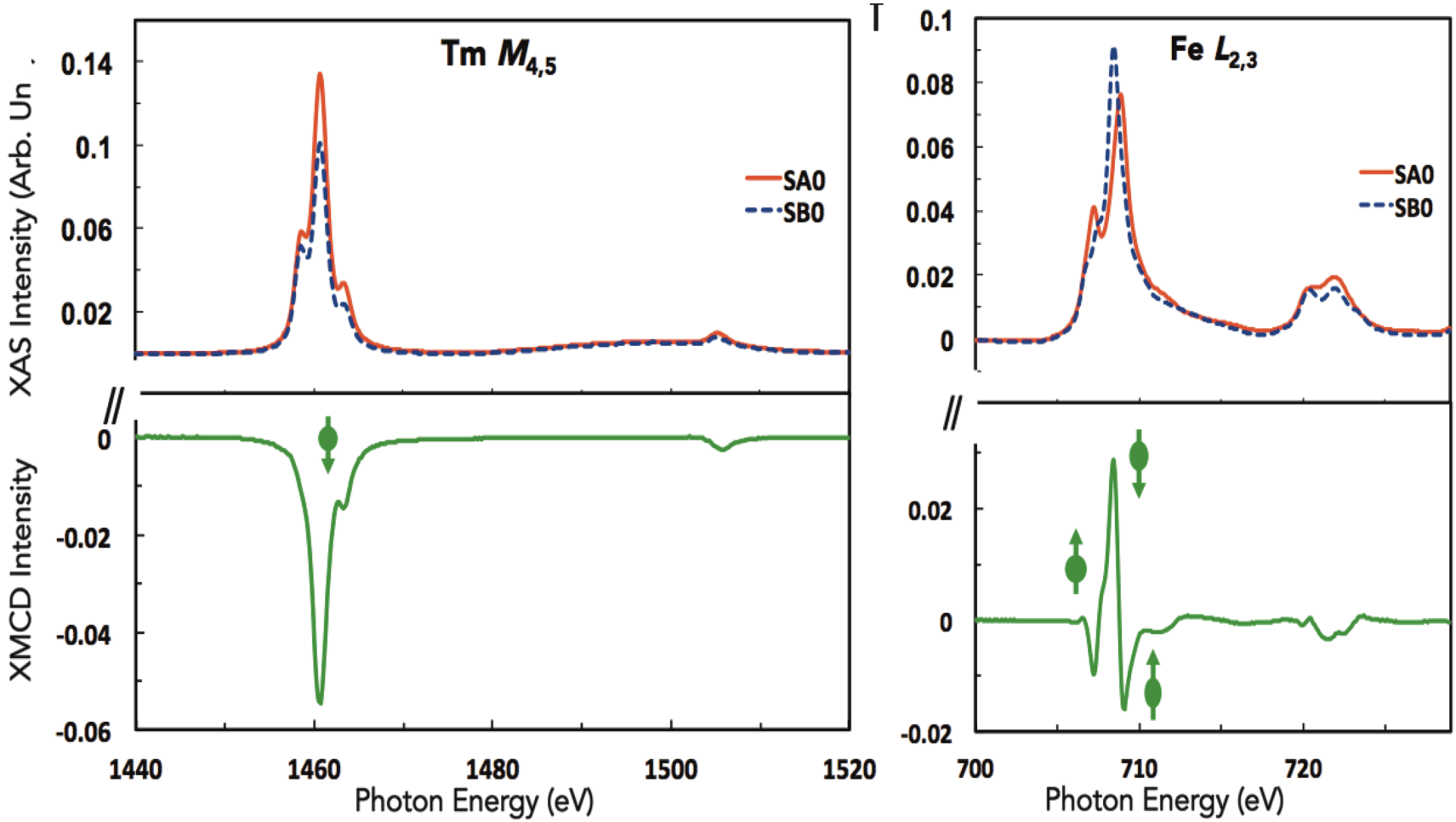

- Tm^{3+} are aligned parallel to octahedral Fe^{3+}, both are antiparallel to tetrahedral Fe^{3+}. Net M parallel to tetrahedral Fe^{3+}.
- Bulk-like. No compensation point down to at least 1.5K ?

Quindeau et al, Adv. Electronic Mater. 1 1600376 (2017) Diamond Light Source, UK

Other iron garnets

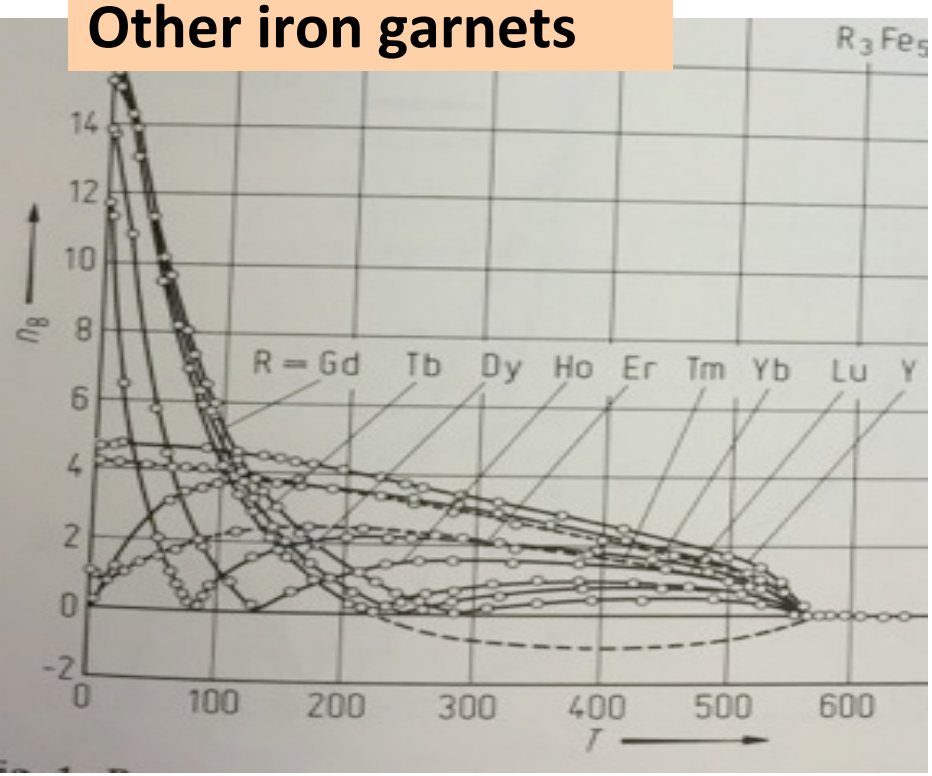

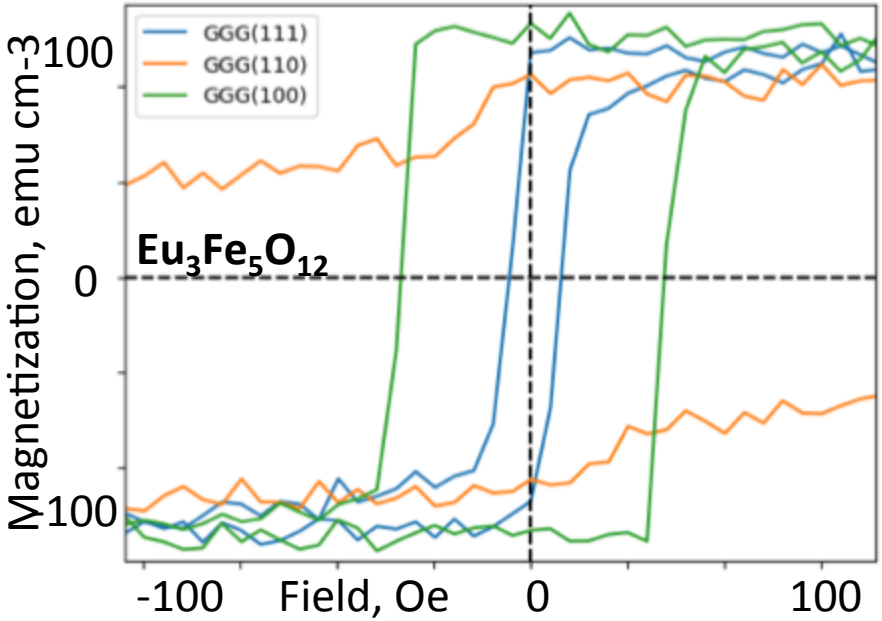

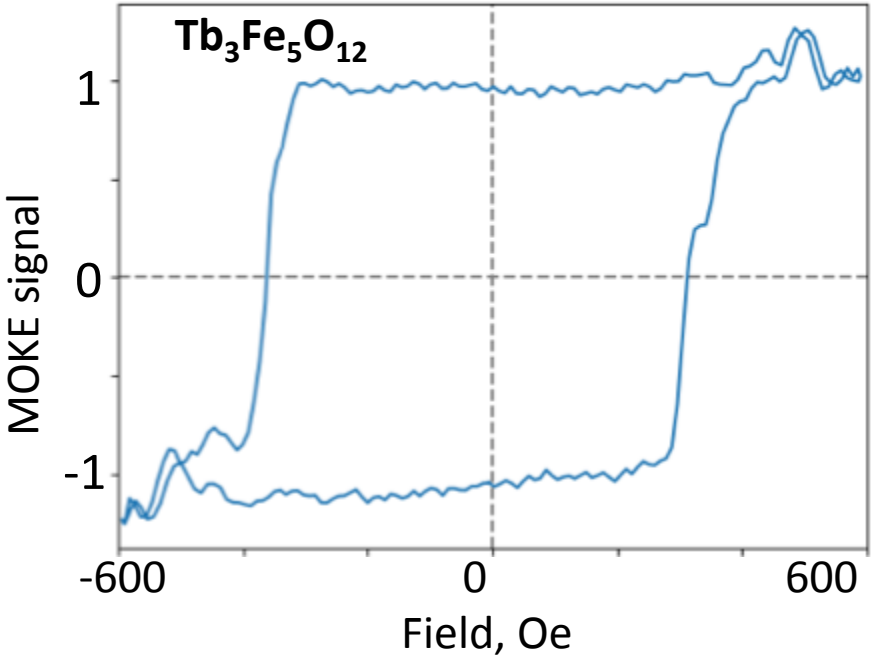

- **TbIG has PMA for (111)** film: in-plane compression, positive λ_{111}
- **EuIG has PMA in (100), (111) and (110) orientations** because λ_{100} and λ_{111} are both positive
- Various compensation temperatures possible including RT – allows arbitrarily small magnetization

Spin orbit torque switching of TmIG (8 nm)/ Pt(5nm)

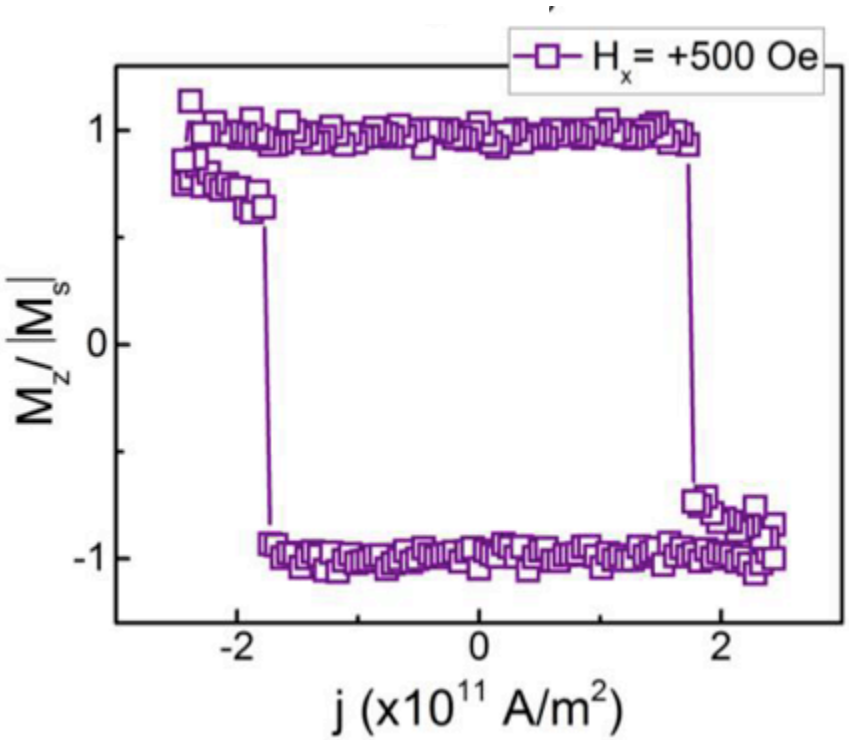

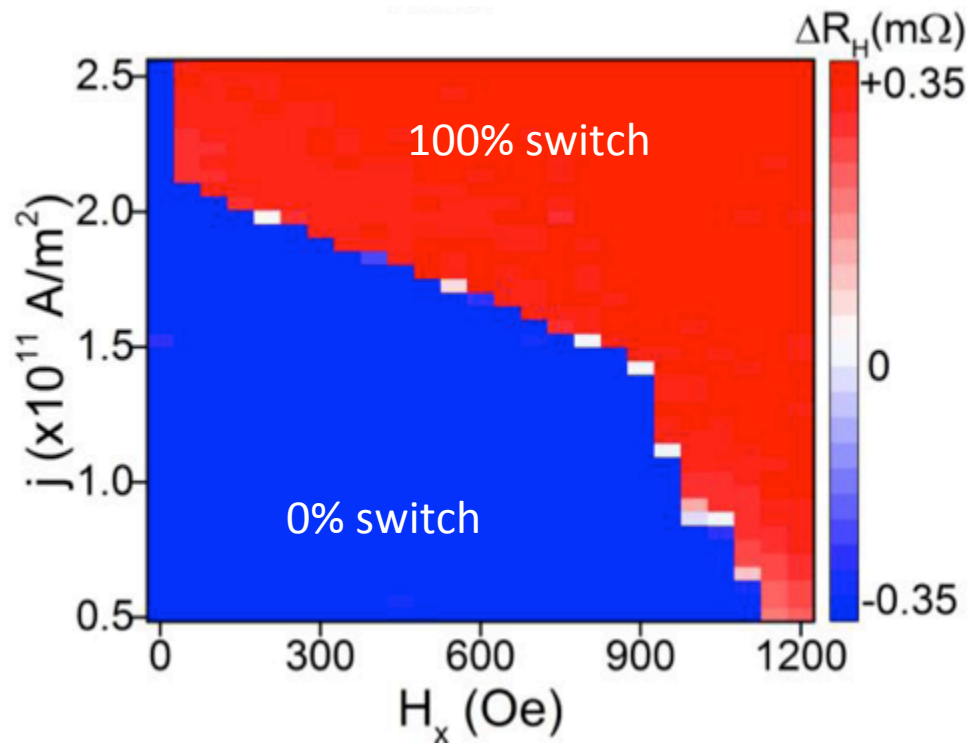

- **Complete switching** observed for TmIG on passing 5 ms current pulse through Pt at j_c = ~ 1-2 x10^{11} A/m^2
- Switching **down to 2 ns pulses**
- Bidirectional switching at fixed in-plane field **as low as 2 Oe**
- **Velocities ~1000 m/s**

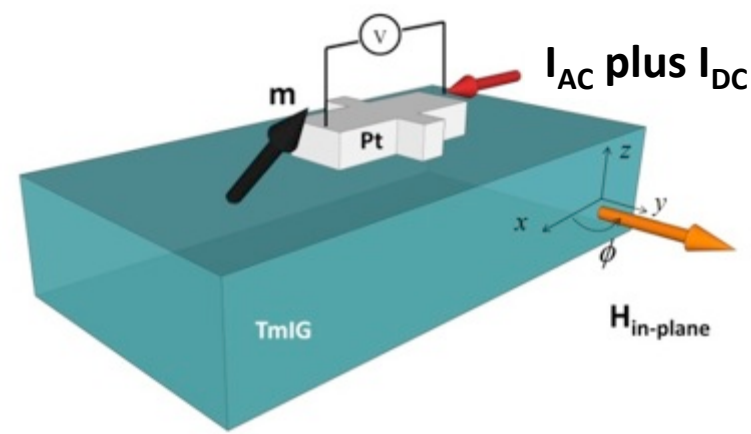

Avci, G. Beach et al, Nature Materials 16 309 (2017)

Proximity-induced Magnetism in Topological Insulator/TmIG

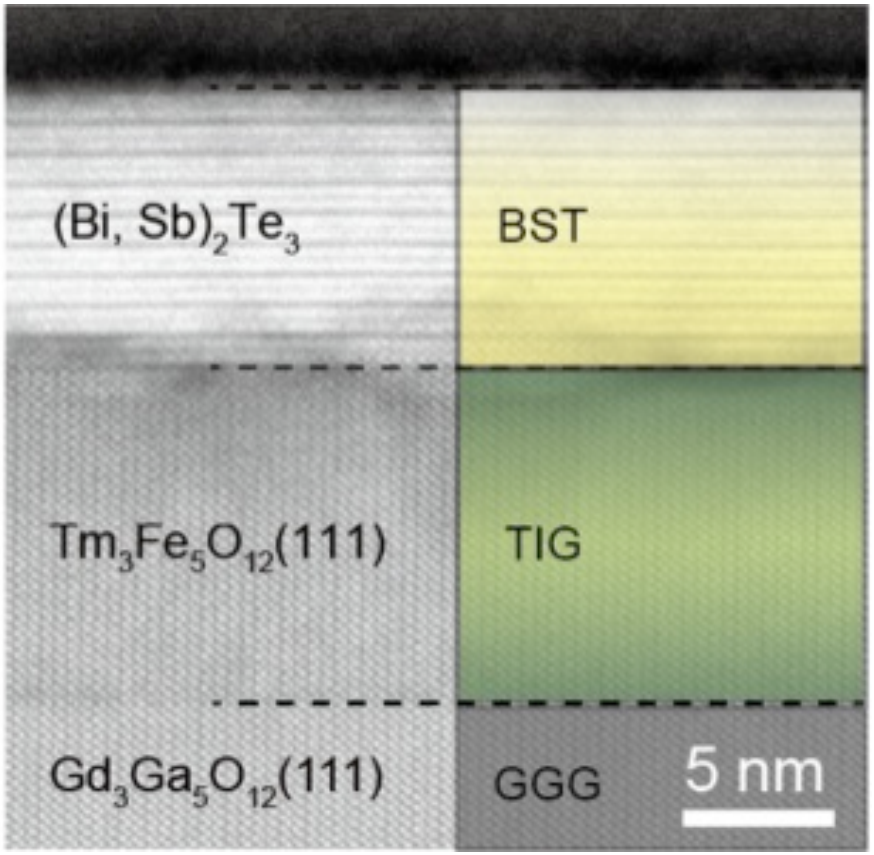

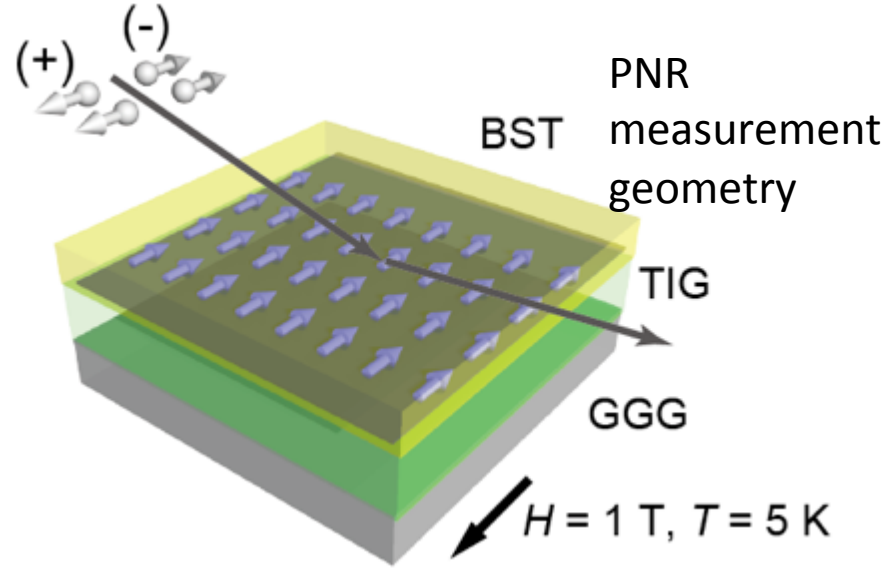

PNR measurement geometry

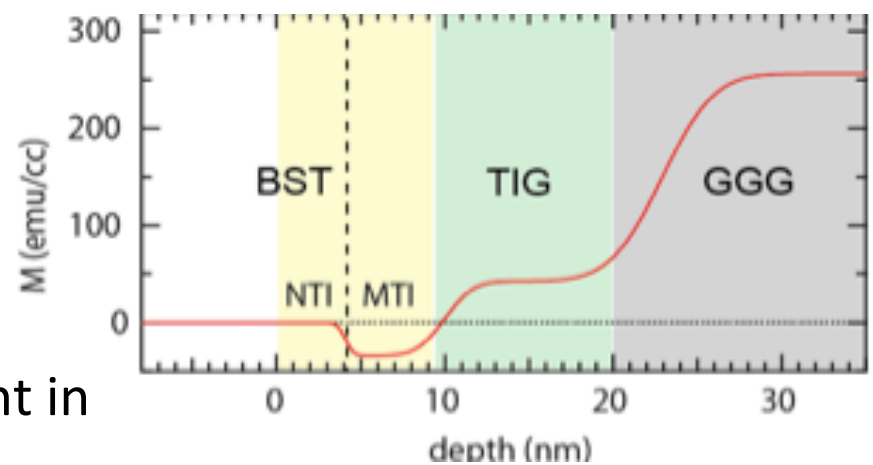

- Proximity-induced magnetic moment in the first ~5 nm of the topological insulator.
- Induced net magnetization in (Bi, Sb)$_2$Te$_3$ antiparallel to TmIG net moment

K. Murata, Kang Wang, UCLA/ ORNL Neutron Source

Magnetic Oxides – Perovskites

Oxygen vacancy effects in $Sr(Ti,Fe)O_{3-\delta}$ on STO or Si

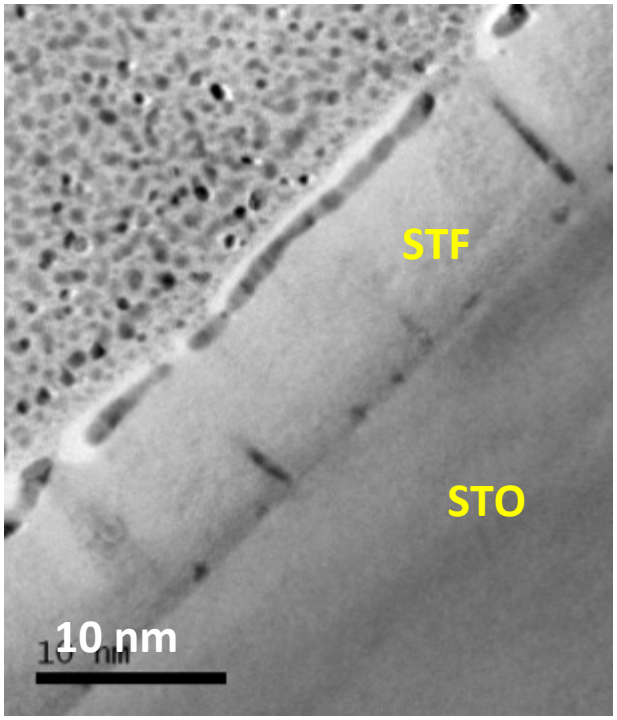

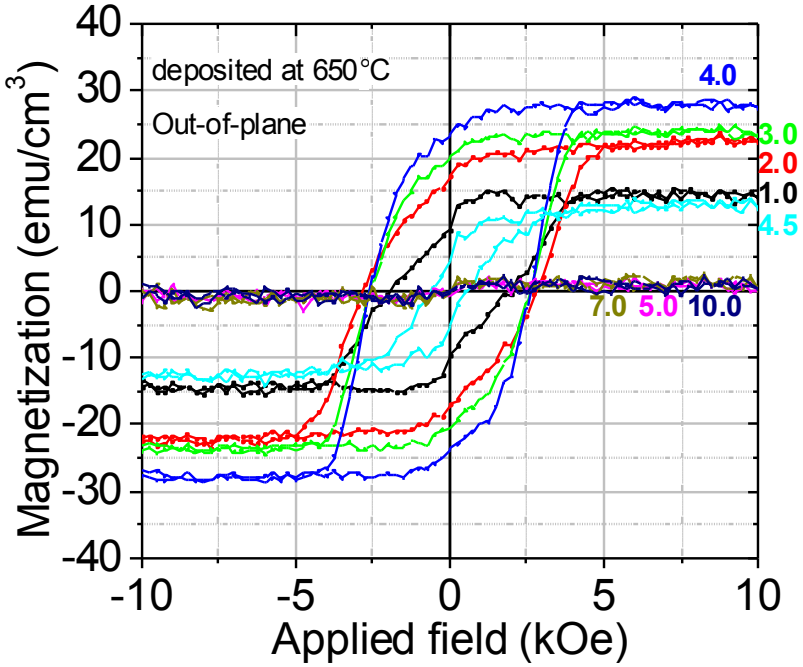

Fe = 35% of Ti sites

- Most Fe is in perovskite lattice (not precipitates)
- STF is magnetic when deposited at low oxygen pressure
- Correlates with unit cell volume
- XMCD (Riccardo Comin, performed at Argonne) correlates with O pressure

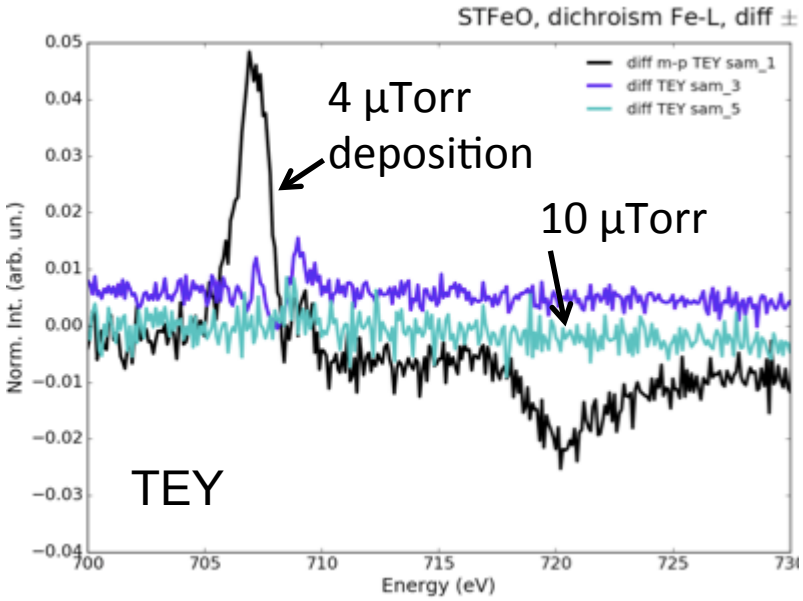

Self-assembled two-phase multiferroic oxides

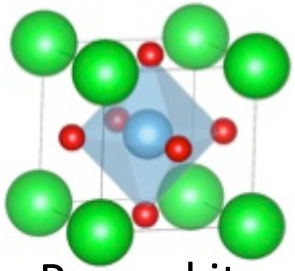

Perovskite: ABO_3

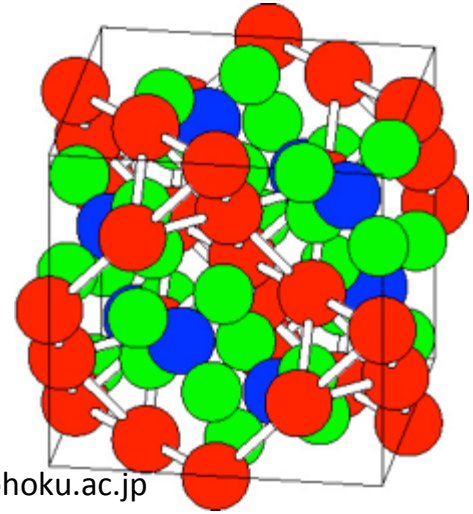

tohoku.ac.jp

Spinel: AB_2O_4

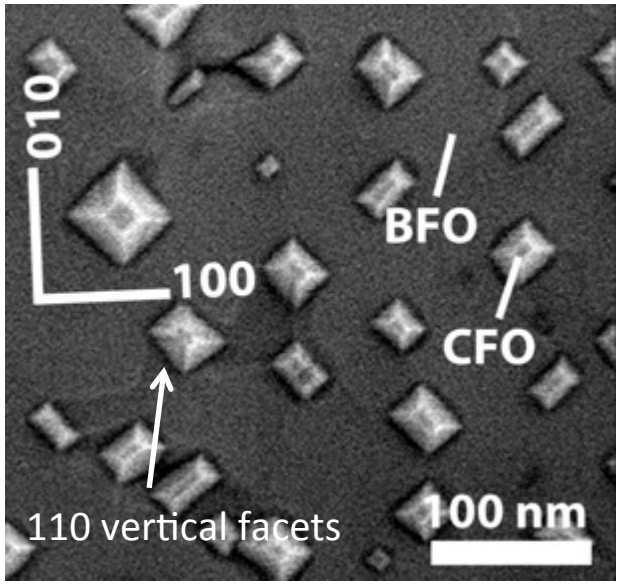

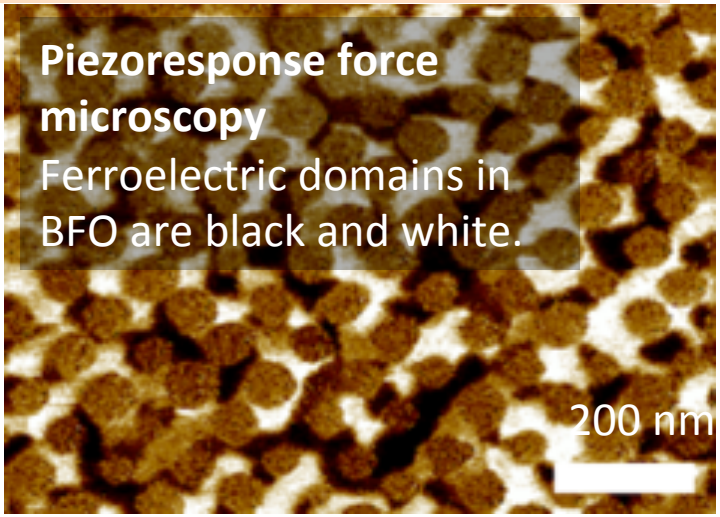

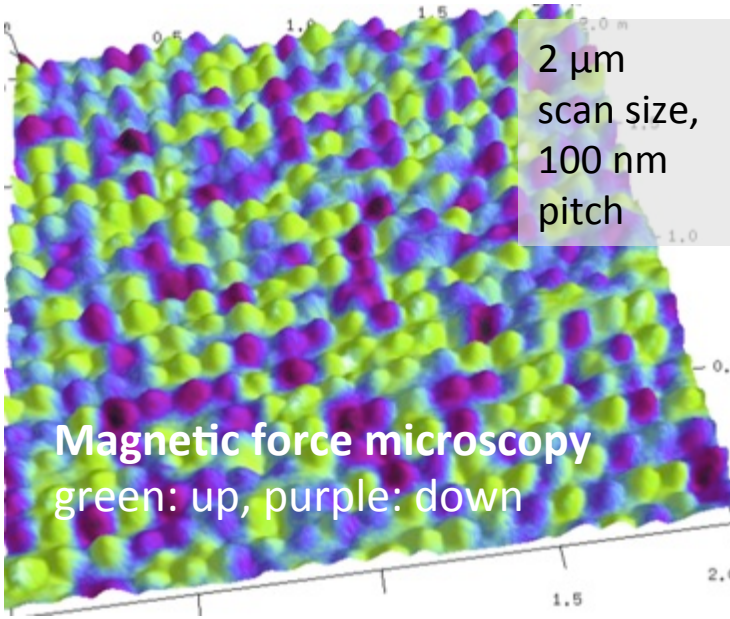

- Co-deposition of immiscible oxides produces a two-phase vertical epitaxial structure.
- **Ferromagnetic + ferroelectric →**
  Magnetoelectric multiferroics
- Interest in oxides: imaging order, domains, stoichiometry; measure coupling, oxygen vacancy effects, piezostrain distribution

Strain-mediated Magnetoelectric effects between piezoelectric BFO and magnetoelastic CFO

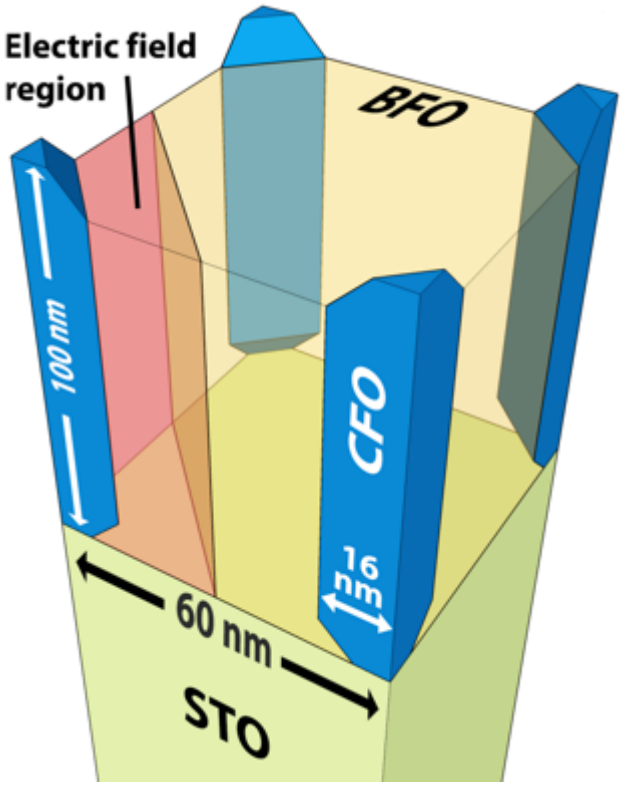

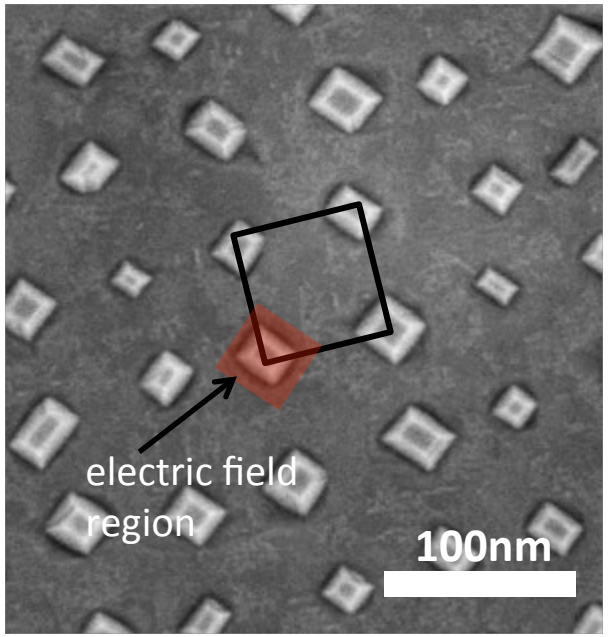

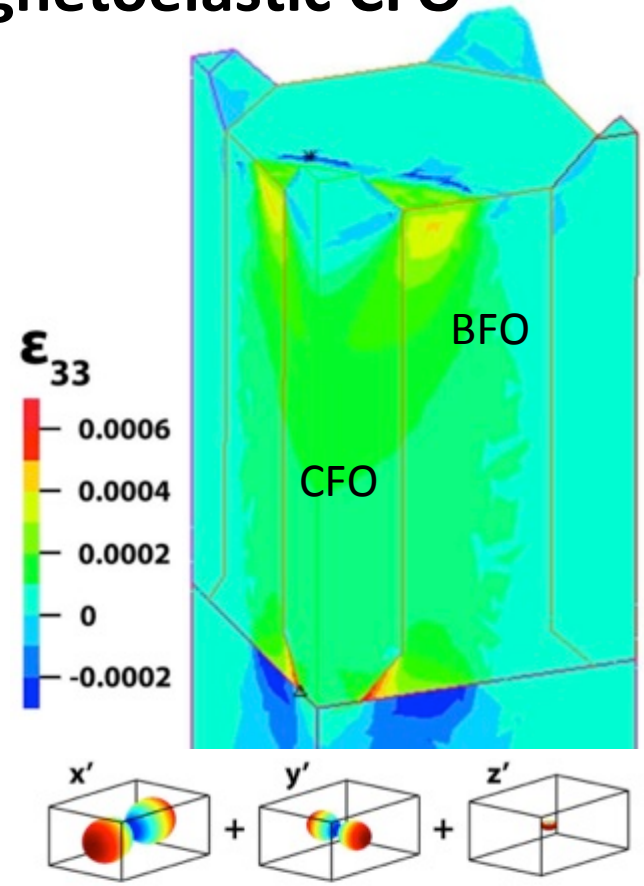

- Piezostrain from BFO is transmitted to CFO.
- Calculate **non-uniform** strain state in CFO then determine magnetoelastic anisotropy.
- Calculate total magnetic anisotropy and use micromagnetics to determine hysteresis of CFO.

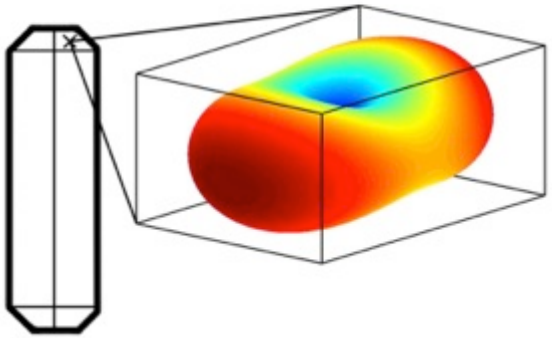

Aimon et al., Appl. Phys. Lett. 101 232901 (2012)

Conclusions

- **Templated Self-assembly of block copolymers** provides a path towards nanolithography
- **GISAXS** reveals details of the microphase separation process in situ for different polymer architectures under solvent (or thermal) annealing
- **Magnetic oxides** (garnets, substituted perovskites or self-assembled spinel-perovskite nanocomposites): magnetic ordering, domains/textures, proximity effects, oxygen vacancy effects. ferroelectric/magnetic coupling may be revealed by beamline studies

Acknowledgements: NSF, SRC, CSPIN Center; Use of MRSEC Shared Facilities